1   **Extracellular ATP facilitates cell extrusion from epithelial layers**

2   **mediated by cell competition or apoptosis**

3

4   Yusuke Mori,[1,2] Naoka Shiratsuchi,[1] Nanami Sato,[1,2] Azusa Chaya,[1] Nobuyuki

5   Tanimura,[1,2] Susumu Ishikawa,[2] Mugihiko Kato,[2] Ikumi Kameda,[2] Shunsuke Kon,[2]

6   Yukinari Haraoka,[3] Tohru Ishitani,[3] and Yasuyuki Fujita[1,2,4*]

7   [1]Department of Molecular Oncology, Graduate School of Medicine, Kyoto

8   University, Yoshida-Konoe-Cho, Sakyo-Ku, Kyoto-city, Kyoto, 606-8501, Japan

9   [2]Division of Molecular Oncology, Institute for Genetic Medicine, Hokkaido

10   University Graduate School of Chemical Sciences and Engineering, Kita-15 Nishi-7,

11   Kita-Ku, Sapporo, 060-0815, Japan

12   [3]Department of Homeostatic Regulation, Division of Cellular and Molecular Biology,

13   Research Institute for Microbial Diseases, Osaka University, 3-1 Yamadaoka, Suita,

14   Osaka, 565-0871, Japan

15   [4]Lead Contact

16   *Correspondence: fujita@monc.med.kyoto-u.ac.jp

17

18

1 **SUMMARY**

2 **For the maintenance of epithelial homeostasis, various aberrant or dysfunctional**

3 **cells are actively eliminated from epithelial layers. This cell extrusion process**

4 **mainly falls into two modes: cell competition-mediated extrusion and apoptotic**

5 **extrusion. However, it is not clearly understood whether and how these processes**

6 **are governed by common molecular mechanisms. In this study, we demonstrate**

7 **that the ROS level is elevated within a wide range of epithelial layers around**

8 **extruding transformed or apoptotic cells. The down-regulation of ROS**

9 **suppresses the extrusion process. Furthermore, ATP is extracellularly secreted**

10 **from extruding cells, which promotes the ROS level and cell extrusion.**

11 **Moreover, the extracellular ATP and ROS pathways positively regulate the**

12 **polarized movements of surrounding cells toward extruding cells in both cell**

13 **competition-mediated and apoptotic extrusion. Hence, extracellular ATP acts as**

14 **an 'extrude me' signal and plays a prevalent role in cell extrusion, thereby**

15 **sustaining epithelial homeostasis and preventing pathological conditions or**

16 **disorders.**

17

18 **KEYWORDS**

21

22

1 INTRODUCTION

2 To preserve its barrier function and structural integrity, the epithelium possesses

3 several homeostatic mechanisms. Among them, cell extrusion is one of the most

4 crucial processes by which aberrant or dysfunctional cells are actively eliminated

5 from epithelial layers to maintain a healthy, homogenous cellular society.[1-5] There are

6 two major types of cell extrusion: cell competition-mediated extrusion and apoptotic

7 extrusion; both phenomena are evolutionarily conserved, at least partly, from flies to

8 mammals. Cell competition is a process through which cells with different properties

9 compete with each other for survival and space; aberrant or dysfunctional cells often

10 become loser cells and are eventually eliminated from tissues, whereas the

11 surrounding normal cells become winner cells that proliferate and fill the vacant

12 spaces.[6-15] It has been demonstrated that normal epithelial cells can recognize and

13 actively eliminate the neighboring oncogenically transformed cells via cell

14 competition, implying that normal epithelia have an anti-tumor activity that does not

15 involve immune cells. This tumor suppressive phenomenon within epithelia is termed

16 epithelial defense against cancer (EDAC).[16,17] In EDAC, transformed cells are

17 eliminated in either cell death-independent or -dependent manner. For instance, in

18 vertebrates, when oncoprotein Ras-, Src-, or ErbB2-transformed cells are surrounded

19 by normal cells, transformed cells are extruded into the apical lumen of the epithelial

20 layer in a cell-death independent fashion.[18-20] In contrast, tumor suppressor protein

21 Scribble- or Lgl (lethal giant larvae)-deficient cells undergo apoptosis when

22 surrounded by normal epithelial cells and are eventually eliminated from epithelia in

23 *Drosophila* and mammals.[21-24] In addition to these cell competition-mediated cell

24 extrusions, when apoptosis is induced independently of cell competition (*e.g.* UV

25 irradiation or caspase activation), the apoptotic cells are extruded from the epithelial

1   layer.[25-28] These different types of cell extrusion are currently regarded as distinct

2   cellular processes, and it remains elusive whether and how common molecular

3   mechanisms are involved in these homeostatic phenomena.

4   When cells receive physical or chemical insults including hypoxia, injury,

5   inflammation, and apoptosis, ATP is often secreted from stressed cells into the

6   extracellular spaces.[29-33] Extracellular ATP can then act as a signaling molecule that

7   binds to membrane receptors P2X or P2Y, thereby affecting multiple cellular

8   processes such as the production of reactive oxygen species (ROS), leading to the

9   maintenance of tissue homeostasis.[31,33] The excess production of ROS can damage

10   cells, whereas the moderate level of ROS can regulate various physiological

11   phenomena such as cell proliferation, metabolism, and motility.[34-36] In this study, we

12   demonstrate that the extracellular ATP and ROS pathways play a prevalent role in cell

13   extrusion.

14

1   **RESULTS**

2

3   **The interaction between normal and RasV12- or Src-transformed cells promotes**

4   **the level of ROS within an epithelial layer**

5   A previous study using the imaginal disc epithelia of *Drosophila* demonstrated that

6   ROS play a role in cell competition.[37] To examine the involvement of ROS in cell

7   competition in mammals, we used CellROX® Orange Reagent, a fluorogenic probe

8   which exhibits bright orange fluorescence upon oxidation by ROS, and Madin-Darby

9   canine kidney (MDCK) epithelial cells stably expressing GFP-RasV12 in a

10   tetracycline-inducible manner.[19] It was previously reported that under the co-culture

11   condition of normal MDCK and RasV12-expressing MDCK cells, at 18-24 h after

12   tetracycline addition, RasV12 cells are apically extruded from a monolayer of normal

13   cells in a cell death-independent manner via cell competition.[19] When normal or

14   RasV12-transformed cells were cultured alone, the level of intracellular ROS

15   remained low (Figures 1A and 1B). In contrast, when normal and RasV12 cells were

16   co-cultured, the ROS level was substantially elevated in both normal and RasV12

17   cells (Figures 1A and 1B). The increased ROS level was observed at 10-16 h after

18   tetracycline addition (Figures 1B and S1A) and under various mix-ratio conditions of

19   normal and RasV12 cells from 1:1 to 2,000:1 (Figure S1B). The increase of the ROS

20   level in the surrounding normal cells was observed further than 160 μm (10-13 cell-

21   length) around most of RasV12 cells (Figure S1C, left), and around some of RasV12

22   cells the ROS level was gradually decreased but retained within 160 μm (Figure S1C,

23   right), demonstrating the increased ROS level over the wide range of surrounding

24   normal cells. When normal and GFP-expressing cells were co-cultured, the up-

25   regulation of ROS did not occur (Figures S1D and S1E). Addition of the ROS

scavenger Trolox profoundly diminished the ROS level in both normal and RasV12

cells (Figures 1C and 1D). In addition, the Trolox treatment significantly suppressed

apical extrusion of RasV12-transformed cells from the epithelial monolayer (Figures

1E and 1F). The ROS level was also elevated in the co-culture of normal and Src-

transformed cells (Figures S1F and S1G), and the Trolox treatment suppressed apical

extrusion of Src cells (Figure S1H). Collectively, these data suggest that ROS play a

crucial role in cell competition-mediated extrusion of transformed cells.

NOX2-mediated ROS production in normal cells facilitates apical extrusion of

RasV12-transformed cells

To explore an upstream regulator of ROS, we examined the effect of various chemical

inhibitors on the ROS level and apical extrusion under the co-culture condition of

normal and RasV12-transformed cells (Table S1). Among the tested inhibitors, the

NADPH oxidase inhibitor VAS2870 significantly suppressed both the ROS level and

apical extrusion (Figures 2A and 2B; Table S1). In mammals, there are seven

NADPH oxidases that are membrane-bound ROS-generating enzymes: NOX1-5 and

DUOX1-2. By quantitative real-time PCR analysis, the NOX2 expression in normal

and RasV12 cells and the NOX4 expression in RasV12 cells were detected, whereas

the expression of the other NADPH oxidases was at an undetectable or very low level

(Figure S2A). To examine the functional role of NOX2 or NOX4, we established

MDCK cells stably expressing NOX2-shRNA (Figure S2B) or RasV12-transformed

MDCK cells stably expressing NOX2- or NOX4-shRNA (Figure S2E). NOX2-

knockdown in normal cells significantly suppressed the ROS level in both normal and

neighboring RasV12 cells (Figures 2C, 2D, and S2C) and diminished the frequency of

1 apical extrusion (Figures 2E and S2D). In contrast, knockdown of NOX2 or NOX4 in

2 RasV12 cells did not affect the ROS level (Figure S2F).

3 In a previous study, we have shown that when RasV12 cells are surrounded by

4 normal cells, the expression of pyruvate dehydrogenase kinase 4 (PDK4) is non-cell-

5 autonomously elevated in RasV12 cells.[38] The increased PDK4 then phosphorylates

6 and inactivates pyruvate dehydrogenase, thereby diminishing the mitochondrial

7 membrane potential, which positively regulates apical extrusion of RasV12 cells.[38]

8 We showed that NOX2-knockdown in normal cells suppressed the PDK4 expression

9 in the co-cultured RasV12 cells (Figure S3A). TMRM (tetramethylrhodamine methyl

10 ester) is a positively charged red fluorescent dye that is incorporated into active

11 mitochondria according to the negative membrane potential gradient across their inner

12 membranes. Using TMRM, we also demonstrated that Trolox treatment or NOX2-

13 knockdown in normal cells profoundly restored the mitochondrial membrane potential

14 in RasV12 cells (Figures S3B-S3E). Collectively, these data indicate that NOX2-

15 induced ROS production in normal cells promotes the expression of PDK4 and

16 decreases mitochondrial activity in the neighboring RasV12 cells, thereby facilitating

17 their apical extrusion.

18

19 **Extracellular ATP signaling is an upstream regulator of ROS**

20 Previous studies have demonstrated that extracellular ATP signaling can activate

21 NADPH oxidase and promote ROS production.[39,40] Indeed, the addition of apyrase, an

22 ecto-ATPase (ATP-diphosphohydrolase) that degrades extracellular ATP into AMP,

23 significantly decreased the ROS level in normal and RasV12-transformed cells under

24 the mix culture condition (Figure 3A and Table S1). In addition, the apyrase treatment

25 suppressed apical extrusion of RasV12 cells (Figure 3B). Extracellular ATP binds and

1   activates purinergic P2X and P2Y receptors.[41,42] The addition of suramin, an

2   antagonist to purinergic P2X and P2Y receptors, suppressed the ROS level and apical

3   extrusion (Figures 3A and 3B; Table S1). To further examine extracellular ATP, we

4   used CellTiter-Glo 2.0, a luminescent indicator for ATP. The amount of extracellular

5   ATP in conditioned media from mono-cultured RasV12 cells was much higher than

6   that from mono-cultured normal cells (Figure 3C). ATP can be released from the

7   cytosol to extracellular space through multiple ATP-permeable channels: volume-

8   regulated anion channels (VRACs), maxi-anion channels (MACs), connexin, and

9   pannexin hemichannels.[43,44] The addition of Gd^{3+} (MACs inhibitor) or 5-Nitro-2-(3-

10   phenylpropylamino) benzoic acid (NPPB) (inhibitor for both VRACs and MACs)

11   reduced the extracellular ATP level in a conditioned medium from RasV12 cells

12   (Figure S4A). In contrast, carbenoxolone (CBX) (inhibitor for both connexins and

13   pannexins) did not affect the extracellular ATP level (Figure S4A). In addition, either

14   Gd^{3+} or NPPB treatment significantly suppressed the ROS level and apical extrusion

15   under the co-culture condition (Figures S4B-S4D). We next examined the effect of

16   exogenously added ATP in a conditioned medium. The exogenous ATP treatment

17   increased the ROS level in normal cells, but not that in NOX2-knockdown normal

18   cells or in RasV12 cells (Figure S4E). In addition, the ATP treatment enhanced apical

19   extrusion of RasV12 cells (Figure S4F). In contrast, exogenous ATP did not induce

20   apical extrusion of GFP cells (Figure S4F), suggesting that the activation of the

21   extracellular ATP pathway alone is not sufficient to cause apical extrusion.

22   Collectively, these results suggest that extracellular ATP released from RasV12 cells

23   through MACs stimulates the production of ROS in normal cells via NOX2, which

24   facilitates apical extrusion.

1 We then analyzed the expression level of purinergic P2X and P2Y receptors in

2 normal or RasV12 cells by quantitative real-time PCR. The expression level of most

3 of the P2 purinergic receptors was lower in RasV12 cells than in normal cells (Figure

4 S4G), which may cause RasV12 cells being insensitive to extracellular ATP (Figure

5 S4E). Among the P2Y and P2X receptors detected in this analysis, P2Y1 and P2Y2

6 promote the activation of NOX2.[45-47] To investigate the functional role of P2Y1 and

7 P2Y2, we established MDCK cells stably expressing P2Y1- or P2Y2-shRNA (Figure

8 S4H). Knockdown of either P2Y1 or P2Y2 in normal cells suppressed the ROS level

9 in both normal and RasV12-transformed cells under the mix culture condition and

10 attenuated the frequency of apical extrusion of RasV12 cells (Figures 3D, 3E, S4I,

11 and S4J). Conversely, knockdown of NOX2 did not significantly affect the expression

12 level of P2Y1 or P2Y2 (Figure S4G). These data suggest that extracellular ATP

13 promotes ROS production and apical extrusion by activating P2Y1 and P2Y2

14 receptors in the surrounding normal cells.

15

16 **Extracellular ATP and ROS pathways positively regulate apical extrusion of**

17 **RasV12-transformed cells in mouse intestinal epithelia**

18 To examine the functional role of the extracellular ATP and ROS pathways in cell

19 extrusion *ex vivo* and *in vivo*, we used cell competition model mouse systems.[38] We

20 crossed a *villin-Cre^ERT2* mouse with an *LSL-eGFP* or *LSL-Ras^V12-IRES-eGFP* mouse

21 and then administrated a low dose of tamoxifen, which induced recombination events

22 less frequently, resulting in the expression of GFP or RasV12-GFP in a mosaic

23 manner within the intestinal epithelia. Using this system, we analyzed the fate of

24 newly emerging RasV12-transformed cells that are surrounded by normal epithelial

25 cells *ex vivo* and *in vivo*. First, we examined the ROS level in intestinal organoids

harboring GFP- or RasV12-expressing cells. The ROS level was profoundly elevated

in both RasV12 and surrounding normal cells within the epithelial layer in organoids

harboring RasV12-expressing cells but not in organoids harboring GFP-expressing

cells (Figures 4A and 4B). In addition, antioxidant Trolox treatment significantly

suppressed apical extrusion of RasV12-transformed cells from intestinal epithelia *ex*

vivo (Figures 4C-4E). Furthermore, we examined the functional involvement of ROS

in the apical elimination of RasV12-transformed cells *in vivo*. 4-Hydroxinonenal (4-

HNE) is a product of lipid peroxidization, which is used as an oxidative stress marker.

The level of 4-HNE was increased in the RasV12-expressing intestinal epithelium

compared with the GFP-expressing intestine (Figure S5A). Administration of Trolox

markedly suppressed the 4-HNE level and apical extrusion of RasV12 cells (Figures

S5B-S5D). We further examined the functional role of extracellular ATP *ex vivo*.

Apyrase treatment profoundly decreased the ROS level in intestinal organoids

harboring RasV12-expressing cells (Figures 4F and 4G). In addition, apyrase

significantly suppressed apical extrusion of RasV12 cells (Figures 4H and 4I).

Collectively, these results indicate that extracellular ATP and ROS play a positive

role in apical extrusion of RasV12-transformed cells in mouse intestinal epithelia as

well.

Extracellular ATP promotes cell competition-mediated extrusion of Scribble-knockdown cells

We next examined whether the extracellular ATP and ROS pathways also play a role

in another type of cell competition-mediated cell extrusion. When tumor suppressor

protein Scribble-mutant/knockdown cells are surrounded by normal cells, cell

competition occurs between these cells, and consequently Scribble-

1 mutant/knockdown cells undergo apoptosis and are extruded from the monolayer of

2 normal epithelial cells.[21,22,48] When Scribble-knockdown MDCK cells were co-

3 cultured with normal MDCK cells, the ROS level was significantly increased in both

4 normal and Scribble-knockdown cells (Figures 5A and 5B), and Trolox treatment

5 reduced the ROS levels (Figures 5C and 5D). In the co-culture of normal and RasV12

6 cells, knockdown of NOX2 in normal cells suppressed the ROS level (Figures 2C and

7 2D). In contrast, in the co-culture of normal and Scribble-knockdown cells, the ROS

8 level was not significantly affected by knockdown of NOX2 in normal cells (Figure

9 S6A), suggesting that under the co-culture of normal and Scribble-knockdown cells,

10 the increase of the ROS level was induced in a NOX2-independent manner. Trolox

11 treatment significantly suppressed the extrusion of Scribble-knockdown cells (Figure

12 5E), suggesting that ROS promote cell competition-mediated extrusion of Scribble-

13 knockdown cells. Next, we further investigated the involvement of extracellular ATP.

14 The amount of extracellular ATP in conditioned media from mono-cultured Scribble-

15 knockdown cells was higher than that from mono-cultured normal cells (Figure 5F).

16 Similarly to RasV12 cells, the addition of Gd^{3+} or NPPB, but not CBX, reduced the

17 extracellular ATP level in a conditioned medium from Scribble-knockdown cells

18 (Figure S6B). Moreover, knockdown of P2Y1 or P2Y2 receptor in normal cells

19 suppressed the ROS level and extrusion of Scribble-knockdown cells under the co-

20 culture condition (Figures 5G and 5H). Collectively, these results suggest that the

21 extracellular ATP and ROS pathways regulate both cell death-independent and -

22 dependent extrusion of transformed cells through cell competition.

23

24 **The extracellular ATP and ROS pathways play a prevalent role in cell extrusion**

1   Previous studies have demonstrated that cells undergoing apoptosis are apically

2   extruded from the epithelial layer in vertebrates.[25] To explore the involvement of the

3   extracellular ATP and ROS pathways in apoptotic cell extrusion, we established

4   MDCK cells stably expressing GFP-tagged caspase-8 in a tetracycline-inducible

5   manner (Figure 6A). In the co-culture of normal and caspase-8-expressing cells,

6   around 6 h after tetracycline addition, caspase-8-expressing cells underwent apoptosis

7   and were apically extruded from the epithelial monolayer (Figure 6B). At 3 h of

8   tetracycline treatment, membrane impermeable SYTOX-dye was not incorporated

9   into caspase-8-expressing cells (Figure S6C), implying that membrane integrity is still

10   maintained at this earlier time point. Under this condition, the extracellular ATP level

11   in conditioned media from caspase-8-expressing cells was higher than that from

12   normal cells (Figure 6C) which was diminished by treatment with apyrase or pan-

13   caspase inhibitor Z-VAD-FMK (Figure S6D), suggesting that ATP is released from

14   caspase-8-expressing cells at the early stage of apoptosis. We found that at 3 h of

15   tetracycline treatment, the ROS level was significantly increased in both normal and

16   caspase-8-expressing cells in the co-culture condition (Figures 6D and 6E). In

17   addition, apyrase treatment significantly suppressed the ROS level (Figures 6F and

18   6G). Furthermore, the ROS level was also decreased by the addition of Trolox or Z-

19   VAD-FMK (Figures 6H and 6I). Moreover, apyrase or Trolox treatment significantly

20   prolonged the extrusion time after induction of caspase-8 expression (Figure 6J).

21   Collectively, these data suggest that extracellular ATP and ROS also promote

22   apoptosis-mediated cell extrusion from the epithelial layer.

23   Caspase-8-expressing cells surrounded by normal cells were often fragmented

24   during cell extrusion, whereas single-cultured caspase-8-expressing cells were

25   apically extruded without fragmentation (Figures S6E and S6F; Video S1). Addition

1   of apyrase or Trolox significantly attenuated the frequency of fragmentation of

2   caspase-8-expressing cells (Figures S6E and S6F; Videos S2 and S3). Addition of

3   apyrase did not substantially affect the timing or intensity of the activation of

4   downstream effector caspase-3 in the extruding cells (Figures S6G and S6H). These

5   data imply that extracellular ATP induces the fragmentation phenotype of extruding

6   apoptotic cells.

7

8   **The extracellular ATP and ROS pathways induce directional movement of**

9   **surrounding normal cells toward extruding cells**

10   Next, we explored the functional significance of the extracellular ATP and ROS

11   pathways in cell extrusion. During cell extrusion, the surrounding cells move toward

12   extruding cells and fill the vacant spaces within epithelial layers, but the underlying

13   molecular mechanism of this process remains elusive. We then analyzed the

14   movement of surrounding cells during apical extrusion (Figure 7A); in the following

15   experiments, we focused on the movement of the surrounding cells at the third row

16   from extruding RasV12-transformed cells or caspase-8-expressing cells. When

17   normal cells were co-cultured with RasV12 cells, the surrounding normal cells moved

18   further distances than normal cells cultured alone (Figure 7B; Video S4). Trolox

19   treatment or NOX2-knockdown in normal cells significantly suppressed the increased

20   cell motility (Figure 7B; Videos S5 and S6). In addition, in the mix culture condition,

21   surrounding normal cells showed polarized movement toward extruding RasV12

22   cells, which was suppressed by Trolox treatment or NOX2 knockdown (Figure 7C;

23   Videos S4-S6). We further investigated the involvement of extracellular ATP in the

24   polarized cell movement of surrounding cells. Apyrase treatment significantly

25   suppressed the motility and directional movement of surrounding cells toward

1   extruding RasV12 cells (Figures 7D and 7E). Moreover, the knockdown of P2Y1 or

2   P2Y2 receptor in normal cells also decreased the polarized movement of surrounding

3   cells (Figures 7D and 7E). Increased cell motility and directional movement of

4   surrounding normal cells were also observed during the extrusion of caspase-8-

5   expressing cells (Figures 7F and 7G). Apyrase or Trolox treatment profoundly

6   suppressed the directional movement of normal cells toward caspase-8-expressing

7   cells (Figures 7F and 7G). Collectively, these results suggest that the extracellular

8   ATP and ROS pathways regulate the polarized movement of the surrounding cells

9   within the epithelial layer during cell competition-mediated and apoptotic extrusion.

1 **DISCUSSION**

2 Previous studies have revealed multiple factors that are involved in the extrusion of

3 aberrant or dysfunctional cells from epithelia. For cell competition-mediated cell

4 extrusion in *Drosophila* or mammals, several groups have identified membrane

5 proteins or soluble proteins that play a key role in the interaction between loser and

6 winner cells, including Flower, Toll-related receptors, SAS/PTP10D, EphA2,

7 SPARC, and FGF21.[49-54] For apoptotic cell extrusion, sphingosine-1-phosphate (S1P)

8 from apoptotic cells or surrounding environments positively regulates the

9 delamination of apoptotic cells from the epithelial layer.[27,55] However, most of these

10 molecules are involved in the extrusion of only certain types of cells, thus it remains

11 elusive whether there are common regulators that harness various types of cell

12 extrusion. In this study, using cell culture and mouse *ex vivo* model systems, we

13 demonstrate that extracellular ATP plays a prevalent role in cell extrusion in

14 mammals. The blockage of the extracellular ATP signaling pathway suppresses both

15 cell competition-mediated extrusion and apoptotic extrusion. ATP is actively secreted

16 from extruding cells, which profoundly influences the surrounding cells, thereby

17 facilitating cell extrusion. Hence, extracellular ATP from extruding cells transmits the

18 'extrude me' signal that promotes their extrusion from epithelial layers (Figure 7H).

19 Previous studies have demonstrated that injured or infected cells secrete ATP which

20 serves as a danger signal to recruit immune cells against tissue damage or infection.[56-

21 58] Similarly, during the extrusion of aberrant cells from epithelial layers, extracellular

22 ATP might act as an alerting signal to inform the neighboring cells of the presence of

23 extruding cells to facilitate the extrusion process for the maintenance of epithelial

24 barrier functions.

1   Our results suggest that Maxi-anion channel (MAC) is involved in the ATP

2   secretion from RasV12- or Scribble-transformed cells, thereby inducing cell

3   competition phenotypes, though we cannot exclude the possibility that ATP may be

4   also secreted through MAC from the surrounding normal cells. The molecular identity

5   of MAC still remains poorly understood. A recent study reported that solute carrier

6   organic anion transporter family member 2a1 (SLCO2A1) is a key component of

7   MAC,[59] though the expression of SLCO2A1 is not detected in MDCK cells (data not

8   shown). The function of MAC is silent at a steady status, but can be activated by

9   physiological or pathological stimuli such as osmotic, hypoxic, or metabolic

10   stresses;[60-63] in particular, the relationship between MAC activity and swelling-

11   induced stress is well-documented [61,63]. Thus, it is plausible that the membrane

12   stretching of extruding cells may trigger the ATP release. Indeed, morphological

13   changes of transformed cells accompanying membrane stretching are observed at the

14   early step of apical extrusion.[19] The regulatory mechanisms for extracellular ATP

15   secretion in cell extrusion need to be further elucidated in future studies.

16   In this study, we have presented data indicating that ROS function downstream of

17   the extracellular ATP signal in the extrusion of both transformed and apoptotic cells.

18   First, treatment with apyrase or suramin, an inhibitor for extracellular ATP signaling,

19   profoundly suppresses the ROS level within an epithelial layer. Second, knockdown

20   of P2Y1 or P2Y2, a receptor for extracellular ATP, also decreases the ROS level.

21   Third, exogenously added ATP increases intracellular ROS. Furthermore, we have

22   also revealed molecular mechanism of how ROS positively regulate cell extrusion.

23   Inhibition of the ROS pathway significantly suppresses the motility of surrounding

24   cells, suggesting that the increased ROS induce the directional movement of

25   surrounding cells toward extruding cells and promote cell extrusion by generating

1   compressive forces onto extruding cells, consistent with previous studies that ROS

2   positively regulate polarized cell motility.[34,64-66] Moreover, knockdown of NOX2 in

3   the surrounding cells also affects the mitochondrial activity in extruding transformed

4   cells. Collectively, these data indicate that the increased ROS within the epithelial

5   layer profoundly influence the behavior of both extruding cells and the surrounding

6   cells, thereby regulating cell extrusion in an orchestrated manner. It is plausible,

7   however, that other downstream regulator(s) of extracellular ATP than ROS may also

8   play a certain role in cell extrusion.

9   Currently, there remain several questions to be answered. First, how do ROS

10   propagate across a wide range of the epithelial layer around extruding cells? Around

11   most of extruding cells, the CellROX fluorescence intensity is comparable between

12   the proximal and distant surrounding cells. Thus, diffusion of extracellular ATP alone

13   may not be sufficient to cause the rather homogenous ROS elevation across the

14   epithelial layer. In addition, an inhibitor for Gap junction or Aquaporin, which

15   potentially blocks intercellular diffusion of ROS, does not affect the ROS level,

16   suggesting that the propagation of ROS within the epithelial layer is not mediated

17   solely by simple diffusion of ROS. Furthermore, exosome inhibitor does not affect the

18   ROS level, either (Table S1). Thus, it remains unknown how ROS are propagated in

19   the extracellular or intercellular spaces. Second, does the increased ROS in extruding

20   cells play a certain role in cell extrusion? Knockdown of NOX2 in the surrounding

21   cells diminishes the ROS level in RasV12 cells, but knockdown of NOX2 or NOX4 in

22   RasV12 cells does not, suggesting that the increased ROS in RasV12 cells are derived

23   from the neighboring cells. To understand the significance of elevated ROS in

24   RasV12 cells, we have tried to establish RasV12 cell lines stably expressing a key

25   anti-oxidant regulator Nrf2, but failed, possibly due to the cytotoxic effect of Nrf2

1   overexpression. Third, is there any functional link between the extracellular ATP and

2   ROS pathways and other regulators for cell extrusion? Calcium wave and actomyosin

3   ring formation play a vital role in the execution of cell extrusion.[25,26] At the final step

4   of cell extrusion, calcium wave propagates from extruding cells across the

5   surrounding cells, which induces the formation of actomyosin rings around extruding

6   cells, thereby generating physical forces required for cell extrusion.[26] As the increased

7   ROS within the epithelial layer are observed at the earlier time point (Figure S6I), it is

8   possible that the extracellular ATP and ROS pathways act upstream of calcium wave

9   or that extracellular ATP regulates both ROS and calcium wave in parallel. In

10   addition to calcium wave, ERK activity waves are also generated around RasV12-

11   expressing cells, which promote the extrusion process.[67] The MEK inhibitor U0126

12   does not affect the ROS level under the mix-culture condition (Table S1), indicating

13   that ERK waves do not act upstream of ROS, but there remains a possibility that

14   secreted extracellular ATP from transformed cells may trigger ERK waves. These

15   issues need to be clarified in future studies.

16   Various types of aberrant cells can be extruded from epithelial layers, including

17   damaged, dysfunctional, transformed, infected, aged, and dead cells.[1-4,68,69] Previous

18   studies have demonstrated that the extrusion/removal of aberrant cells is required for

19   proper embryonic development and also prevents ageing and tissue degeneration in

20   the adult.[68,70-72] Thus, the dysregulation of cell extrusion processes would potentially

21   cause a variety of pathological conditions or disorders by accumulating abnormal or

22   harmful cells within epithelial tissues. Hence, the further elucidation of molecular

23   mechanisms for cell extrusion could lead to clinical applications for the maintenance

24   of tissue homeostasis and improvement of human health.

25

12

13 **AUTHOR CONTRIBUTIONS**

14 Y.M. designed experiments and generated most of the data. N.Sh., N.Sa., A.C., N.T.,

15 S.I., M.K., I.K., S.K, Y.H., and T.I. assisted experiments. Y.F. conceived and

16 designed the study. The manuscript was written by Y.M., N.Sh., and Y.F. with

17 assistance from the other authors.

18

19 **DECLARATION OF INTERESTS**

20 The authors declare no competing interests.

21

1

FIGURE LEGENDS

3

Figure 1. Up-regulated ROS by the interaction of normal and RasV12-transformed cells promote apical extrusion

(A and B) The intracellular ROS level in the single- or co-culture of normal and RasV12-transformed cells. Normal MDCK cells and MDCK-pTR GFP-RasV12 cells were cultured alone or co-cultured at a ratio of 50:1, and the intracellular ROS level was examined by CellROX. (A) CellROX fluorescent images. (B) Quantification of fluorescent intensity of CellROX. Values are expressed as a ratio relative to single-cultured MDCK cells. Data are mean ± SD from four independent experiments. $*p < 0.05$, $**p < 0.01$, and NS: not significant (one-way ANOVA with Tukey's test); $n = 373, 364, 234$, and 585 cells.

(C and D) Effect of antioxidant Trolox on the intracellular ROS level. MDCK-pTR GFP-RasV12 cells were co-cultured with normal MDCK cells at a ratio of 1:50 in the absence or presence of Trolox. (C) CellROX fluorescent images. (D) Quantification of fluorescent intensity of CellROX. Values are expressed as a ratio relative to single-cultured MDCK cells. Data are mean ± SD from three independent experiments. $*p < 0.05$ (one-way ANOVA with Dunnett's test); $n = 235, 260, 166, 403, 154$, and 313 cells.

(E and F) Effect of antioxidant Trolox on apical extrusion of RasV12-transformed cells. (E) The xz-immunofluorescent images of MDCK-pTR GFP-RasV12 cells surrounded by normal MDCK cells in the absence or presence of Trolox. (F) Quantification of apical extrusion of RasV12-transformed cells surrounded by normal

1 cells. Data are mean ± SD from four independent experiments. *p < 0.05 (paired two-

2 tailed Student's t-test); n = 523 and 524 cells.

3 (A, C, and E) Scale bars, 20 μm.

4 See also Figure S1.

5

6 **Figure 2. NOX2 in surrounding normal cells positively regulates ROS**

7 **production, thereby promoting apical extrusion of RasV12-transformed cells**

8 (A and B) Effect of the NADPH oxidase inhibitor VAS2870 on the intracellular ROS

9 level in normal or RasV12-transformed cells (A) and apical extrusion of RasV12 cells

10 (B). (A) Quantification of fluorescent intensity of CellROX. Normal MDCK cells and

11 MDCK-pTR GFP-RasV12 cells were cultured alone or co-cultured at a ratio of 50:1

12 in the absence or presence of VAS2870, followed by CellROX analysis. Values are

13 expressed as a ratio relative to single-cultured MDCK cells. Data are mean ± SD from

14 four independent experiments. *p < 0.05 (one-way ANOVA with Dunnett's test); n =

15 175, 155, 156, 345, 130, and 272 cells. (B) Quantification of apical extrusion of

16 RasV12-transformed cells. Data are mean ± SD from three independent experiments.

17 *p < 0.05 (paired two-tailed Student's t-test); n = 377 and 416 cells.

18 (C and D) Effect of NOX2-knockdown in surrounding normal cells on the

19 intracellular ROS level. MDCK-pTR GFP-RasV12 cells were co-cultured with

20 normal MDCK cells or MDCK NOX2-shRNA1 cells at a ratio of 1:50, followed by

21 CellROX analysis. (C) CellROX fluorescent images. Scale bar, 20 μm. (D)

22 Quantification of fluorescent intensity of CellROX. Values are expressed as a ratio

23 relative to single-cultured MDCK cells. Data are mean ± SD from five independent

24 experiments. *p < 0.05 (one-way ANOVA with Tukey's test); n = 300, 302, 300, 279,

25 789, 236, and 547 cells.

1   (E) Effect of NOX2-knockdown in surrounding normal cells on apical extrusion of

2   RasV12-transformed cells. Data are mean ± SD from three independent experiments.

3   *$p < 0.05$ (paired two-tailed Student's t-test); $n = 324$ and 299 cells.

4   See also Figures S2 and S3.

5

6   **Figure 3. Extracellular ATP positively regulates the intracellular ROS level and**

7   **apical extrusion**

8   (A and B) Effect of apyrase or suramin on the intracellular ROS level (A) and apical

9   extrusion (B). (A) Quantification of fluorescent intensity of CellROX. Normal MDCK

10   cells and MDCK-pTR GFP-RasV12 cells were cultured alone or co-cultured at a ratio

11   of 50:1 in the absence or presence of apyrase or suramin, followed by CellROX

12   analysis. Values are expressed as a ratio relative to single-cultured MDCK cells. Data

13   are mean ± SD from four (right two) or five (left six) independent experiments. *$p <$

14   0.05 and **$p < 0.01$ (one-way ANOVA with Dunnett's test); $n = 300$, 300, 328, 880,

15   228, 638, 206, and 556 cells. (B) Quantification of apical extrusion of RasV12-

16   transformed cells. Data are mean ± SD from three independent experiments. *$p < 0.05$

17   (one-way ANOVA with Dunnett's test); $n = 327$, 407, and 446 cells.

18   (C) Measurement of the extracellular ATP level in conditioned media. The

19   extracellular ATP level in conditioned media from normal MDCK or MDCK-pTR

20   GFP-RasV12 cells cultured alone was measured using CellTite-Glo 2.0 reagent. Data

21   are mean ± SD from five independent experiments. *$p < 0.05$ (paired two-tailed

22   Student's t-test).

23   (D and E) Effect of P2Y1- or P2Y2-knockdown in surrounding normal cells on the

24   intracellular ROS level (D) and apical extrusion (E). (D) Quantification of fluorescent

25   intensity of CellROX. Normal MDCK, MDCK P2Y1-shRNA1, or MDCK P2Y2-

1   shRNA1 cells were cultured alone or co-cultured with MDCK-pTR GFP-RasV12

2   cells at a ratio of 50:1, followed by CellROX analysis. Values are expressed as a ratio

3   relative to single-cultured MDCK cells. Data are mean ± SD from three independent

4   experiments. *p < 0.05, **p < 0.01, and ***p < 0.001 (one-way ANOVA with

5   Dunnett's test); n = 160, 159, 149, 162, 203, 449, 140, 288, 110, and 239 cells. (E)

6   Quantification of apical extrusion of RasV12-transformed cells surrounded by normal,

7   P2Y1-knockdown, or P2Y2-knockdown cells. Data are mean ± SD from three

8   independent experiments. *p < 0.05 and **p <0.01 (one-way ANOVA with Dunnett's

9   test); n = 332, 361, and 335 cells.

10 See also Figure S4.

11

12 **Figure 4. Extracellular ATP and ROS promote apical elimination of RasV12-**

13 **transformed cells in mouse intestinal organoids**

14 (A and B) The intracellular ROS level in mouse intestinal organoids harboring

15 RasV12-expressing cells. Intestinal organoids from *villin-Cre^{ERT2}-LSL-eGFP* or *-LSL-*

16 *Ras^{V12}-IRES-eGFP* mice were treated with 100 nM tamoxifen for 24 h, followed by

17 CellROX analysis. (A) Fluorescent images of intestinal organoids stained with

18 CellROX. (B) Quantification of fluorescent intensity of CellROX. Values are

19 expressed as a ratio relative to control (tamoxifen non-treated organoids). Data are

20 mean ± SD from three independent experiments. ***p < 0.001 and NS: not significant

21 (one-way ANOVA with Dunnett's test); n= 122, 101, 132, 115, 90, and 136 cells.

22 (C-E) Effect of Trolox on apical extrusion of RasV12-expressing cells in intestinal

23 organoids. Intestinal organoids from *villin-Cre^{ERT2}-LSL-Ras^{V12}-IRES-eGFP* mice were

24 incubated with 100 nM tamoxifen in the absence or presence of Trolox for 24 h. (C)

25 Immunofluorescent images of intestinal organoids harboring RasV12-expressing

1   cells. The arrowhead or arrows indicate apically extruded or extruding RasV12-

2   expressing cells, respectively. Ap or Ba stands for the apical or basal side of the

3   epithelium, respectively. (D) Classification of the phenotypes of RasV12-expressing

4   cells. 'apically extruded': completely detached from the basement membrane and

5   translocated into the apical side. 'apically extruding': with their nucleus apically

6   shifted, but still attached to the basement membrane. 'not extruded': remaining within

7   the epithelium. (E) Quantification of the phenotypes of RasV12-expressing cells in

8   intestinal organoids treated with Trolox. Data are mean ± SD from three independent

9   experiments. *$p < 0.05$, **$p < 0.01$, and ***$p < 0.001$ (unpaired two-tailed Student's

10 t-test); n = 156 (DMSO-treated organoids) or 134 (Trolox-treated organoids) cells.

11 (F and G) Effect of apyrase on the intracellular ROS level in intestinal organoids

12 harboring RasV12-expressing cells. Intestinal organoids from *villin-Cre^{ERT2}-LSL-*

13 *Ras^{V12}-IRES-eGFP* mice were incubated with 100 nM tamoxifen in the absence or

14 presence of apyrase for 24 h, followed by CellROX analysis. (F) Fluorescent images

15 of intestinal organoids stained with CellROX after apyrase treatment. (G)

16 Quantification of fluorescent intensity of CellROX. Values are expressed as a ratio

17 relative to control (non-treated with tamoxifen or apyrase). Data are mean ± SD from

18 three independent experiments. ***$p < 0.01$ (unpaired two-tailed Student's t-test); n =

19 140, 102, 163, 73, and 123 cells.

20 (H and I) Effect of apyrase on apical extrusion of RasV12-transformed cells in

21 intestinal organoids. Intestinal organoids from *villin-Cre^{ERT2}-LSL-Ras^{V12}-IRES-eGFP*

22 mice were incubated with 100 nM tamoxifen in the absence or presence of apyrase for

23 24 h. (H) Immunofluorescent images of intestinal organoids treated with apyrase. The

24 arrowhead or arrows indicate apically extruded or extruding RasV12-expressing cells,

25 respectively. (I) Quantification of the phenotypes of RasV12-expressing cells in

1   intestinal organoids treated with apyrase. Data are mean $\pm$ SD from three independent

2   experiments. *$p < 0.05$ and **$p < 0.01$ (unpaired two-tailed Student's t-test); n = 190

3   (water-treated) and 171 (apyrase-treated) cells.

4   (A, C, F, and H) Scale bars, 20 μm.

5   (C, F, and H) Stars in the images indicate mucin-rich autofluorescent materials in the

6   apical lumen.

7   See also Figure S5.

8

9   **Figure 5. Extracellular ATP and ROS promote extrusion of Scribble-knockdown**

10   **cells surrounded by normal cells**

11   (A and B) The intracellular ROS level in single- or co-cultured normal and Scribble-

12   knockdown cells. Normal MDCK cells or MDCK-pTR Scribble-shRNA1 cells were

13   cultured alone or co-cultured at a ratio of 10:1, followed by CellROX analysis. (A)

14   CellROX fluorescent images. (B) Quantification of fluorescent intensity of CellROX.

15   Values are expressed as a ratio relative to single-cultured MDCK cells. Data are mean

16    $\pm$ SD from six independent experiments. *$p < 0.05$ and NS: not significant (one-way

17   ANOVA with Tukey's test); n = 355, 350, 349, and 891 cells.

18   (C-E) Effect of Trolox on the intracellular ROS level (C and D) and extrusion of

19   Scribble-knockdown cells surrounded by normal cells (E). (C) CellROX fluorescent

20   images. MDCK-pTR Scribble-shRNA1 cells were co-cultured with normal MDCK

21   cells at a ratio of 1:10 in the absence or presence of Trolox, followed by CellROX

22   analysis. (D) Quantification of fluorescent intensity of CellROX. Values are

23   expressed as a ratio relative to single-cultured MDCK cells. Data are mean $\pm$ SD from

24   four independent experiments. **$p < 0.01$ (one-way ANOVA with Dunnett's test); n

25   = 235, 235, 238, 556, 209, and 458 cells. (E) Quantification of the extrusion of

Scribble-knockdown cells surrounded by normal cells after Trolox treatment. Data are

mean ± SD from three independent experiments. *p < 0.05 (paired two-tailed

Student's t-test); n = 372 and 516 cells.

(F) Measurement of the extracellular ATP level in conditioned media. The

extracellular ATP level in conditioned media from normal MDCK or MDCK-pTR

Scribble-shRNA1 cells cultured alone was measured using CellTite-Glo 2.0 reagent.

Data are mean ± SD from four independent experiments. *p < 0.05 (paired two-tailed

Student's t-test).

(G and H) Effect of P2Y1- or P2Y2-knockdown in surrounding normal cells on the

intracellular ROS level (G) and the extrusion of Scribble-knockdown cells (H). (G)

Quantification of fluorescent intensity of CellROX. MDCK-pTR Scribble-shRNA1

cells were co-cultured with normal MDCK, MDCK P2Y1-shRNA1, or MDCK P2Y2-

shRNA1 cells at a ratio of 1:10, followed by CellROX analysis. Values are expressed

as a ratio relative to single-cultured MDCK cells. Data are mean ± SD from six

independent experiments. **p < 0.01 (one-way ANOVA with Dunnett's test); n = 360,

346, 350, 345, 433, 935, 391, 719, 352, and 754 cells. (H) Quantification of the

extrusion of Scribble-knockdown cells surrounded by normal, P2Y1-knockdown, or

P2Y2-knockdown cells. Data are mean ± SD from four independent experiments. *p

< 0.05 and **p < 0.01 (one-way ANOVA with Dunnett's test); n = 502, 723, and 716

cells.

(A and C) Scale bars, 20 μm.

See also Figure S6.

Figure 6. Extracellular ATP promotes apoptotic extrusion of caspase-8-

expressing cells

(A) Establishment of a tetracycline-inducible caspase-8-expressing MDCK cell line.

Tetracycline-induced expression of GFP-caspase-8 protein and the effect on the

activation of downstream caspase-3 were analyzed by western blotting with the

indicated antibodies.

(B) Representative image of apically extruded caspase-8-expressing cells from an

epithelial layer of normal cells. MDCK-pTR GFP-caspase-8 cells were co-cultured

with normal MDCK cells at a ratio of 1:50, followed by tetracycline treatment for 6 h.

(C) Measurement of the extracellular ATP level in conditioned media. The

extracellular ATP level in conditioned media from normal MDCK or MDCK-pTR

GFP-caspase-8 cells cultured alone was measured using CellTiter-Glo 2.0 reagent.

Data are mean ± SD from four independent experiments. $*p < 0.05$ (paired two-tailed

Student's t-test).

(D and E) The intracellular ROS level in single- or co-cultured normal and caspase-8-

expressing cells. Normal MDCK cells and MDCK-pTR GFP-caspase-8 cells were

cultured alone or co-cultured at a ratio of 50:1, followed by CellROX analysis. (D)

CellROX fluorescent images. (E) Quantification of fluorescent intensity of CellROX.

Values are expressed as a ratio relative to single-cultured MDCK cells. Data are mean

± SD from four independent experiments. $*p < 0.05$, $**p < 0.01$, and NS: not

significant (one-way ANOVA with Tukey's test); n = 240, 230, 157, and 456 cells.

(F-I) Effect of apyrase, Trolox, or Z-VAD-FMK on the intracellular ROS level in co-

cultured normal and caspase-8-expressing cells. Normal MDCK cells and MDCK-

pTR GFP-caspase-8 cells were cultured alone or co-cultured at a ratio of 50:1 in the

absence or presence of apyrase (F and G), Trolox, or Z-VAD-FMK (H and I),

followed by CellROX analysis. (F and H) CellROX fluorescent images. (G and I)

Quantification of fluorescent intensity of CellROX. Values are expressed as a ratio

relative to single-cultured MDCK cells. Data are mean ± SD from four independent

experiments. *p < 0.05 and **p < 0.01 (one-way ANOVA with Dunnett's test); (G) n

= 240, 230, 151, 401, 155, and 385 cells. (I) n = 230, 220, 149, 394, 161, 347, 169,

and 368 cells.

(J) Effect of apyrase or Trolox on extrusion time of caspase-8-expressing cells.

MDCK-pTR GFP-caspase-8 cells were co-cultured with normal MDCK cells at a

ratio of 1:50 in the absence or presence of apyrase or Trolox. Red bars indicate

median values. ***p < 0.001 (Mann-Whitney test); n= 87, 89, 72, and 87 cells from

two independent experiments.

(B, D, F, and H) Scale bars, 20 μm.

See also Figure S6.

**Figure 7. Extracellular ATP and ROS promote directional movement of
surrounding normal cells toward extruding cells**

(A) Analysis of distance and direction of cell migration. The schematic diagram for

the directional movement of surrounding cells toward extruding cells. The yellow

arrow denotes the movement of a surrounding cell. Angle (θ) is measured between

two lines: a solid line linking the centroids of a surrounding cell at the start and end of

the observation (t0 and t1) and a dashed line linking the centroid of a surrounding and

extruding cell at t0. Arrow length and angle indicate the distance and direction of the

cell movement, respectively.

(B and C) Effect of Trolox or NOX2-knockdown on the migration of normal cells

surrounding RasV12-transformed cell. Normal MDCK cells or MDCK NOX2-

shRNA1 cells were cultured alone or co-cultured with MDCK-pTR GFP-RasV12

cells at a ratio of 50:1 in the absence or presence of Trolox. (B) Total distance of

1 migration of normal cells or NOX2-knockdown cells for 6 h. Data are mean ± SD

2 from three independent experiments. *p < 0.05 (one-way ANOVA with Dunnett's

3 test); n = 90 cells for all conditions. (C) Analysis of directional movement of normal

4 cells or NOX2-knockdown cells toward RasV12-transformed cells. Data are mean ±

5 SD from three independent experiments. *p < 0.05 (one-way ANOVA with Dunnett's

6 test); n = 90 cells for all conditions.

7 (D and E) Effect of inhibition of extracellular ATP signaling on the migration of

8 normal cells toward RasV12-transformed cell. Normal MDCK, MDCK P2Y1-

9 shRNA1, or MDCK P2Y2-shRNA1 cells were cultured alone or co-cultured with

10 MDCK-pTR GFP-RasV12 cells at a ratio of 50:1 in the absence or presence of

11 apyrase. (D) The total distance of cell migration of normal cells, P2Y1-knockdown, or

12 P2Y2-knockdown cells for 6 h. Data are mean ± SD from three independent

13 experiments. ***p < 0.001 (one-way ANOVA with Dunnett's test); n = 90 cells for

14 all conditions. (E) Analysis of directional movement of normal cells, P2Y1-

15 knockdown, or P2Y2-knockdown cells toward RasV12-transformed cells. Data are

16 mean ± SD from three independent experiments. *p < 0.05 (one-way ANOVA with

17 Dunnett's test); n = 90 cells for all conditions.

18 (F and G) Effect of inhibition of the extracellular ATP and ROS pathways on the

19 migration of normal cells toward caspase-8-expressing cells. Normal MDCK cells

20 were cultured alone or co-cultured with MDCK-pTR GFP-caspase-8 cells at a ratio of

21 50:1 in the absence or presence of apyrase or Trolox. (F) Total distance of migration

22 of normal cells for 2 h. Data are mean ± SD from three independent experiments. *p <

23 0.05 (one-way ANOVA with Tukey's test); n = 90 cells for all conditions. (G)

24 Analysis of directional movement of normal cells toward caspase-8-expressing cells

25 in the absence or presence of apyrase or Trolox. Data are mean ± SD from three

1   independent experiments. $*p < 0.05$ and $***p < 0.001$ (unpaired two-tailed Student's

2   t-test); n = 90 cells for all conditions.

3   (H) A schematic model of cell extrusion induced by extracellular ATP and ROS

4   pathways.

5

1

STAR METHODS

RESOURCE AVAILABILITY

4

Lead contact

Further information and requests for resources and reagents should be directed to and

will be fulfilled by the lead contact, Yasuyuki Fujita (fujita@monc.med.kyoto-

u.ac.jp).

9

Materials availability

Plasmids or cell lines generated in this study will be made available on request, but

we may require payment and/or a completed Materials Transfer Agreement if there is

potential for commercial application.

14

Data and code availability

・ Data reported in this paper will be shared by the lead contact upon request.

・ This paper does not report the original code.

・ Any additional information required to reanalyze the data reported in this paper is

available from the lead contact upon request.

20

EXPERIMENTAL MODEL AND SUBJECT DETAILS

22

Cell line

MDCK (Madin-Darby canine kidney) cells were cultured in Dulbecco's modified

Eagle's medium (DMEM) supplemented with 10% fetal bovine serum (FBS) (Sigma-

1 Aldrich), 1% penicillin/streptomycin (Life Technologies), and 1% GlutaMax (Life

2 Technologies) in a humidified 5% CO_2 incubator at 37°C. The parental MDCK cells

3 were a gift from W. Birchmeier (MDC, Berlin). Mycoplasma contamination was

4 regularly tested for all cell lines using MycoAlert Mycoplasma Detection kit (Lonza).

5

6 **Animal model**

7 All animal experiments were conducted under the guidelines of the Animal Care

8 Committee of Kyoto University. The animal protocols were reviewed and approved

9 by the Animal Research Committee of Graduate School of Medicine, Kyoto

10 University (MedKyo21059). 6-12-week old *villin/Cre^{ERT}; LoxP-STOP-LoxP*

11 *(LSL)/HRas^{V12}-IRES-eGFP* (a C57BL/6 genetic background) and *villin/Cre^{ERT};*

12 *LSL/eGFP* mice (a C57BL/6 genetic background) of either sex were used in this

13 study. All mice were bred and/or maintained under a 14 h light /10 h dark cycle with

14 food and water available at all times at the Institute of Laboratory Animals, Graduate

15 School of Medicine, Kyoto University.

16

17 **METHOD DETAILS**

18

19 **Antibodies and materials**

20 Rabbit anti-Cleaved Caspase-3 (Asp175) (#9661) antibody was purchased from Cell

21 Signaling Technology. Mouse anti-β-actin (MAB1501R clone C4) and mouse anti-

22 GFP (#11814460001) (used for western blotting) antibodies were from Merck

23 Millipore. Chicken anti-GFP (ab13970) (used for immunohistochemistry) and rabbit

24 anti-4-hydroxynonenal (ab46545) antibodies were from Abcam. Rat anti-E-cadherin

25 (131900) antibody was from Life Technologies. Horseradish peroxidase-conjugated

1   AffiniPure anti-mouse and anti-rabbit IgG were from Jackson ImmunoResearch.

2   Alexa-Fluor-568-conjugated phalloidin (Life Technologies) was used at 1.0 unit/mL.

3   Alexa-Fluor-488-, -568-, and -647-conjugated secondary antibodies were from Life

4   Technologies. Hoechst 33342 (Life Technologies) was used at a dilution of 1:5,000.

5   The inhibitors Z-VAD-FMK (100 μM), CK666 (100 μM), (S)-(-)-blebbistatin

6   (30 μM), LY294002 (10 μM), Y27632 (20 μM), and SMIFH2 (25 μM) were from

7   Calbiochem. CCCP (5 μM), ibuprofen (10 μM), α-Glycyrrhetinic acid (α-GA; 50

8   μM), silver nitrate (50 μM), apyrase (1 unit/mL), carbenoxolone disodium salt (50

9   μM), VAS2870 (1 μM), BAPTA-AM (25 μM), 5-Nitro-2-(3-

10   phenylpropylamino)benzoic acid (NPPB; 50 μM), Gadolinium (III) chloride

11   hexahydrate (10 μM), GW4869 (20 μM), and nocodazole (200 μg/mL) were from

12   Sigma-Aldrich. Trolox (1 mM) and H-89 dihydrochloride (20 μM) were from

13   Cayman Chemical. BAY117082 (1 μM), suramin sodium (10 μM), and ML141 (20

14   μM) were from Santa Cruz Biotechnology. U0126 (10 μM) was from Promega.

15   GsMTx (10 μM) was from PEPTIDE INSTITUTE. ATP disodium salt hydrate (1

16   mM) was from Sigma-Aldrich. Type I collagen (Cellmatrix® Type I-A and

17   Cellmatrix® Type I-P) was obtained from Nitta Gelatin and was neutralized on ice

18   according to the manufacturer's instructions. The SiR-actin Kit (far-red silicon

19   rhodamine (SiR)-actin fluorescence probe) was obtained from SPIROCHROME to

20   stain F-actin and was used according to the manufacturer's instructions.

21

22   **Establishment of cell lines and cell culture**

23   MDCK cells stably expressing GFP (MDCK-pTR GFP), GFP-RasV12 (MDCK-pTR

24   GFP-RasV12), GFP-cSrcY527F (MDCK-pTR GFP-SrcY527F), or Scribble-short

1 hairpin RNA (shRNA) (MDCK-pTR Scribble-shRNA1) in a tetracycline-inducible

2 manner were established and cultured as previously described.[19,21,73] To establish

3 MDCK-pTR GFP-caspase-8 cells, MDCK-pTR cells were transfected with

4 pcDNA4/TO/eGFP-human-caspase-8 by nucleofection using Nucleofector 2b

5 (Lonza), followed by selection in the medium containing 5 μg/mL of blasticidin

6 (Invitrogen) and 400 μg/mL of zeocin (Invitrogen). To establish MDCK cells stably

7 expressing NOX2-shRNA, P2Y1-shRNA, P2Y2-shRNA, or luciferase-shRNA as well

8 as MDCK-pTR GFP-RasV12 cells stably expressing NOX2-shRNA or NOX4-

9 shRNA, each shRNA oligonucleotide was cloned into BglII/XhoI sites of

10 pSUPER.neo (Oligoengine). Sequences of shRNA oligonucleotides are shown in the

11 key resources table. MDCK cells were transfected with pSUPER.neo-NOX2-shRNA,

12 -P2Y1-shRNA, -P2Y2-shRNA, or -luciferase-shRNA by nucleofection, followed by

13 selection in the medium containing 800 μg/mL of Geneticin (G418; Gibco). MDCK-

14 pTR GFP-RasV12 cells were transfected with pSUPER.neo-NOX2-shRNA or -

15 NOX4-shRNA by nucleofection, followed by selection in the medium containing 5

16 μg/mL of blasticidin, 400 μg/mL of zeocin, and 800 μg/mL of G418. For tetracycline-

17 inducible MDCK cell lines, 2 μg/mL of tetracycline (Sigma-Aldrich) was used to

18 induce the expression of proteins or shRNAs.

19

20 **Immunofluorescence and western blotting**

21 For immunofluorescence analysis, MDCK, MDCK NOX2-shRNA, MDCK P2Y1-

22 shRNA, MDCK P2Y2-shRNA, or MDCK luciferase-shRNA cells were mixed with

23 MDCK-pTR GFP-RasV12, MDCK-pTR GFP-cSrcY527F, or MDCK-pTR GFP-

24 caspase-8 cells at a ratio of 50:1 and plated onto collagen-coated coverslips as

25 previously described.[19] The mixture of cells was incubated for 8-12 h, followed by

1   tetracycline treatment for 24 h, except for the analysis of extrusion of SrcY527F-

2   transformed cells or caspase-8-expressing cells, in which cells were examined at 18 h

3   or 6 h after tetracycline treatment, respectively. The indicated inhibitor was added

4   together with tetracycline. After incubation with tetracycline, cells were fixed with

5   4% paraformaldehyde (PFA) in phosphate-buffered saline (PBS) and permeabilized

6   as previously described.[18] For immunofluorescence using intestinal organoids, cells

7   grown in matrigels were incubated with Cell Recovery Solution (Corning) for 8 min

8   before fixation with 4% PFA. After fixation, cells were permeabilized in 0.5% Triton

9   X-100/PBS for 1 h and incubated with 1% bovine serum albumin (BSA)/PBS for 1 h.

10   For immunohistochemical analysis of the small intestine, mice were perfused with 1%

11   PFA. The isolated tissues were fixed with 1% PFA in PBS for 24 h and embedded in

12   FSC 22 Clear Frozen Section Compound (Leica Biosystems). 10-mm-thick frozen

13   sections were cut using Leica CM3050S cryostat (Leica Biosystems). The sections

14   were incubated with 1 x Block-Ace (DS Pharma Biomedical) and 0.1% Triton X-100

15   in PBS for 1 h, followed by incubation with primary or secondary antibody diluted in

16   PBS containing 0.1 x Block-Ace and 0.1% TritonX-100 for 2 h or 1 h respectively at

17   room temperature. All primary antibodies were used at 1:100 except for mouse

18   intestinal tissues: anti-GFP (1:1,000), anti-E-cadherin (1:2,000), and anti-4-

19   hydroxynonenal (1:100) antibodies. All secondary antibodies were used at 1:200 for

20   cultured cells and 1:1,000 for mouse intestinal tissues, respectively.

21   Immunofluorescence images were analyzed with Olympus FV1000 or FV1200 using

22   the Olympus FV10-ASW software. Images were quantified with the MetaMorph

23   software (Molecular Devices) and the Image J software. To monitor the intracellular

24   ROS level in cultured cells, MDCK-pTR GFP, MDCK-pTR GFP-RasV12, MDCK-

25   pTR GFP-cSrcY527F, MDCK-pTR Scribble-shRNA1, or MDCK-pTR GFP-caspase-

1 8 cells were mixed with non-transformed MDCK cells and plated on collagen-coated

2 35-mm glass-bottom dishes and cultured for 8-12 h, followed by addition of

3 tetracycline. Inhibitors were added together with tetracycline. For the inhibition of

4 apoptosis, cells were treated with Z-VAD-FMK for 2 h before tetracycline addition.

5 At 3 h (for caspase-8 cells), 12 h (for SrcY527F cells), 16 h (for RasV12 cells and

6 GFP cells), or 36 h (for Scribble-knockdown cells) after tetracycline addition, cells

7 were incubated with 5 μM CellROX (Invitrogen) for 30 min according to the

8 manufacturer's instructions. After labeling, images of twelve randomly selected fields

9 (2,048 x 2,048 pixels) were captured using a phase-contrast microscope. To monitor

10 the mitochondrial membrane potential, cells were loaded with 50 nM TMRM

11 (Thermo Fisher Scientific) for 30 min and observed as previously described.[38] For

12 Figure S6C, to monitor the membrane integrity of cultured cells, 1.0×10^6 MDCK

13 cells or MDCK-pTR GFP-caspase-8 cells were seeded on collagen-coated 35-mm

14 glass-bottom dishes and cultured for 8-12 h, followed by the treatment of tetracycline

15 for 3 or 6 h. Cells were then incubated with 0.5 μM SYTOX Orange Nucleic Acid

16 Stain (Thermo Fisher Scientific) for 10 min, and images were captured as described

17 above. Western blotting was performed as previously described.[74] Primary and

18 secondary antibodies were used at 1:1,000. Western blotting data were analyzed using

19 ImageQuant™ LAS4010 (GE healthcare).

20

21 **Time-lapse observation of cultured cells**

22 For live-cell imaging, cells were incubated in the Leibovitz's L-15 medium (Gibco)

23 containing 10% FBS. Time-lapse images were captured and analyzed by Nikon

24 confocal microscopy (A1 HD25) with the NIS-Elements software (Nikon). Acquired

25 data were analyzed by the Image J software. For the analysis of the cell movement

1   around RasV12 cells, 5.0 x 10^5 MDCK, MDCK NOX2-shRNA1, MDCK P2Y1-

2   shRNA1, or MDCK P2Y2-shRNA1 cells were co-cultured with MDCK-pTR GFP-

3   RasV12 cells at a ratio of 50:1 on the collagen-coated 35-mm glass-bottom dishes for

4   6 h. Cells were then cultured in the medium containing the far-red silicon rhodamine

5   (SiR)-actin fluorescence probes for 24 h until time-lapse observation started.

6   Tetracycline was added to the medium 8 h before the start of time-lapse imaging.

7   Time-lapse imaging was performed for 6 h to examine the cell movement. For the

8   analysis of the effect of Trolox or apyrase on the cell movement, the inhibitor was

9   added together with tetracycline. Cell movement was measured by tracking the

10   centroids of surrounding cells every hour, and the cumulative distance for 6 h was

11   shown as total distance of cell migration. The angle of directional movement of

12   surrounding cells was calculated based on centroids of RasV12-transformed cells and

13   surrounding cells as demonstrated in Figure 7A. For the analysis of apoptotic cell

14   extrusion, 8.0 x 10^4 MDCK cells were co-cultured with MDCK-pTR GFP-caspase-8

15   cells at a ratio of 50:1 on the collagen-coated 8-well glass-bottom plates (Thermo

16   Fisher Scientific) for 8-16 h. The indicated inhibitor and tetracycline were then added

17   together to the medium. After 2 h of the inhibitor and tetracycline addition, apoptotic

18   cell extrusion was analyzed by time-lapse imaging for 24 h. For analyses of the

19   extrusion time of caspase-8-expressing cells, the time zero was defined as the time

20   when the GFP intensity exceeded 1.1 times as the background fluorescence intensity.

21   Fragmentation of caspase-8-expressing cells upon extrusion was determined using

22   bright-field images of time-lapse observation. For the analysis of the cell movement

23   around caspase-8-expressing cells, surrounding cells were analyzed for 2 h until

24   membrane blebbing was observed in caspase-8-expressing cells. For the analysis of

25   extrusion of Scribble-knockdown cells, 4.0 x 10^5 MDCK, MDCK P2Y1-shRNA1, or

1 MDCK P2Y2-shRNA1 cells were co-cultured with MDCK-pTR Scribble-shRNA1

2 cells at a ratio of 10:1 on the collagen-coated 35-mm glass-bottom dishes for 8 h.

3 Cells were then treated with tetracycline for 36 h. After 36 h of tetracycline treatment,

4 time-lapse analysis was performed for 24 h. For the analysis of the effect of Trolox on

5 the extrusion of Scribble-knockdown cells, Trolox was added into culture media after

6 24 h of tetracycline treatment. Extrusion of Scribble-knockdown cells was determined

7 by the obvious morphological change using bright-field images. To monitor the

8 activity of caspase-3 in cultured cells in live imaging, MDCK cells were co-cultured

9 with MDCK-pTR GFP-caspase-8 cells at a ratio of 50:1 on the collagen-coated 8-well

10 glass-bottom dishes for 8-16 h. Nucview 530 Caspase-3 substrate (2 μM) (Biotium)

11 was then added together with tetracycline and apyrase. After 2 h of the treatment, the

12 activity of caspase-3 was analyzed by time-lapse imaging for 24 h.

13

14 **Quantitative real-time PCR**

15 For quantitative real-time PCR, the indicated cells were seeded at a density of 1×10^6

16 cells on a 6-well plate (Corning). After incubation with tetracycline for 16 h, total

17 RNA was extracted using TRIzol (Thermo Fisher Scientific) and reverse transcribed

18 using QuantiTect Reverse Transcription (Qiagen). qPCR reactions were performed

19 with GeneAce SYBR qPCR Mix (NIPPON GENE) using the StepOne system

20 (Thermo Fisher Scientific). For the analysis of the *PDK4* expression in RasV12-

21 transformed cells, 2×10^7 MDCK or MDCK NOX2-shRNA1 cells were mixed with

22 MDCK-pTR GFP-RasV12 cells at a ratio of 10:1 and seeded on collagen-coated 15-

23 cm dishes (Greiner-Bio-One) as previously described.[38] After incubation with

24 tetracycline for 16 h, GFP-positive RasV12 cells and GFP-negative MDCK cells were

25 separated using an analytical flow cytometer (SH800S, SONY). Relative

1   quantification analysis was performed with the comparative CT method ($2^{-\Delta\Delta CT}$) using

2   *β-actin* as a reference gene to normalize data. The primer sequences are shown in the

3   key resources table.

4

5   **Measurement of the extracellular ATP level**

6   For the measurement of the extracellular ATP level in conditioned media of cultured

7   cells, 1.0×10^6 MDCK cells, MDCK-pTR GFP-RasV12 cells, or MDCK-pTR GFP-

8   caspase-8 cells were seeded on collagen-coated 35-mm dish (Greiner) and incubated

9   for 12 h. Culture media were then changed to FBS-free DMEM containing

10   tetracycline and the indicated inhibitor, followed by the measurement after 3 h (for

11   MDCK-pTR GFP-caspase-8) or 16 h (for MDCK-pTR GFP-RasV12). For Scribble-

12   knockdown cells, 4.0×10^5 MDCK-pTR Scribble-shRNA1 cells were seeded and

13   treated as described above except that following 12 h incubation after seeding, cells

14   were treated with tetracycline for 24 h, and culture media were changed to FBS-free

15   DMEM containing tetracycline and the indicated inhibitor, followed by the

16   measurement after 12 h. For the effect of Z-VAD-FMK, caspase-8-expressing cells

17   were pretreated with Z-VAD-FMK for 2 h prior to tetracycline addition. Collected

18   conditioned media were centrifuged at 111 x g for 5 min at 4°C, and 100 µL of

19   supernatant were transferred into a white opaque 96-well plate (Thermo Fisher

20   Scientific). After 100 µL of CellTiter-Glo 2.0 reagent (Promega) was added into the

21   96-well plate, the plate was horizontally shaken for 2 min and incubated for 10 min at

22   room temperature. After the incubation, the luminescence was measured using

23   Varioskan Flash (Thermo Fisher Scientific). The calibration of luminescence to ATP

24   concentration was performed using ATP standard solutions of known concentration.

25

1   **Mice**

2   *Villin-Cre^{ERT2}* mice were crossed with *CAG-loxP-STOP-loxP (LSL)-eGFP* mice or

3   *DNMT1-CAG-LSL-HRas^{V12}-IRES-eGFP* mice to generate *villin-CreERT2-LSL-eGFP*

4   (*villin-GFP*) mice or *-LSL-HRas^{V12}-IRES-eGFP* (*villin-RasV12-GFP*) mice,

5   respectively.[38] 6-12-week old C57BL/6 mice of either sex were used. For PCR

6   genotyping of mice, primer sequences were as follow; Villin-CreERT2: 5'-

7   CAAGCCTGGCTCGACGGCC-3' and 5'-CGCGAACATCTTCAGGTTCT-3',

8   DNMT1-CAG-loxP-STOP-loxP-HRasV12-IRES-eGFP: 5'-

9   CACTGTGGAATCTCGGCAGG-3' and 5'-GCAATATGGTGGAAAATAAC-3',

10   and CAG-loxP-STOP-loxP-eGFP: 5'-CAGTCAGTTGCTCAATGTACC-3' and 5'-

11   ACTGGTGAAACTCACCCA-3'. *Villin-RasV12-GFP* or *villin-GFP* mice were given

12   a single intraperitoneal injection of 1 or 0.5 mg of tamoxifen, respectively, in corn oil

13   (Sigma) per 20 g of body weight, and mice were then sacrificed at 3 days after Cre

14   activation. To examine the effect of Trolox on oxidative stress in intestinal epithelia,

15   *villin-RasV12-GFP* mice were first administrated with 50 mg/kg of Trolox (Sigma-

16   Aldrich) in corn oil by intraperitoneal injection at days 0 and 2. Subsequently, the

17   mice were injected intraperitoneally with 1.0 mg of tamoxifen at day 3. After 24 h of

18   tamoxifen injection, the mice were intraperitoneally administrated with 50 mg/kg of

19   Trolox at days 4 and 5 and then sacrificed at day 6. To culture intestinal organoids,

20   isolated crypts from the mouse small intestine were entrapped in matrigel (Corning)

21   and plated in a non-coated 35-mm glass-bottom dish as previously described.[38] The

22   crypts embedded in matrigel were covered with cultured media (Advanced

23   DMEM/F12, Gibco) supplemented with N2 (Invitrogen), B27 (Invitrogen), 50 ng/mL

24   EGF (PeproTech), 100 ng/mL Noggin (PeproTech), 1.25 mM N-acetylcysteine

25   (NAC) (Sigma-Aldrich), and the R-spondin conditioned medium collected from

1   293T-HA-Rspol-Fc cells provided by Dr. Calvin Kuo (Stanford University). After

2   96 h culture, organoids were incubated in the culture media without B27 and NAC

3   and treated with 100 nM tamoxifen (Sigma) for 24 h to induce transgenes.

4   Subsequently, tamoxifen was washed out, and organoids were incubated with

5   CellROX for 1 h or fixed with 4% PFA. To examine the effect of Trolox or Apyrase

6   *ex vivo*, organoids were incubated in the culture medium without B27 and NAC and

7   were treated with 100 nM tamoxifen in the absence or presence of Trolox or apyrase

8   for 24 h.

9

10   **QUANTIFICATION AND STATICAL ANALYSIS**

11

12   **Statistics analysis**

13   To compare the difference between two groups, unpaired or paired two-tailed

14   Student's *t*-tests were conducted. For multiple comparisons, one-way ANOVA with

15   Dunnett's test or Tukey's test was performed. Mann-Whitney test was conducted in

16   Figures 6J and S6H. P-values less than 0.05 were considered to be significant. No

17   statistical method was used to predetermine sample size.

18

1 **Video S1. Apoptotic cell extrusion of caspase-8-expressing cells surrounded by**

2 **normal cells, related to Figure 6**

3 Figure S6H (left) shows a cropped image from this movie. Normal MDCK cells were

4 co-cultured with MDCK-pTR GFP-caspase-8 cells at a ratio of 50:1. Images were

5 captured at 5-min intervals. Scale bar, 20 μm.

6

7 **Video S2. Effect of apyrase on apoptotic extrusion of caspase-8-expressing cells**

8 **surrounded by normal cells, related to Figure 6**

9 Figure S6H (right) shows a cropped image from this movie. Normal MDCK cells

10 were co-cultured with MDCK-pTR GFP-caspase-8 cells at a ratio of 50:1 in the

11 presence of apyrase. Images were captured at 5-min intervals. Scale bar, 20 μm.

12

13 **Video S3. Effect of Trolox on apoptotic cell extrusion of caspase-8-expressing**

14 **cells surrounded by normal cells, related to Figure 6**

15 Normal MDCK cells were co-cultured with MDCK-pTR GFP-caspase-8 cells at a

16 ratio of 50:1 in the presence of Trolox. Images were captured at 5-min intervals. Scale

17 bar, 20 μm.

18

19 **Video S4. Directional movement of surrounding cells toward RasV12-**

20 **transformed cells, related to Figure 7**

21 Normal MDCK cells were co-cultured with MDCK-pTR GFP-RasV12 cells at a ratio

22 of 50:1, followed by the treatment with tetracycline for 8 h, and then cell movement

23 of surrounding cells was observed by time-lapse imaging for 6 h. The trajectories of

24 the centroid of surrounding cells are shown as colored lines. Images were captured at

25 15-min intervals. Scale bar, 20 μm.

1

Video S5. Effect of Trolox on the directional movement of surrounding cells

toward RasV12-transformed cells, related to Figure 7

Normal MDCK cells were co-cultured with MDCK-pTR GFP-RasV12 cells at a ratio

of 50:1, followed by the treatment with tetracycline and Trolox for 8 h, and then cell

movement of surrounding cells was observed by time-lapse imaging for 6 h. The

trajectories of the centroid of surrounding cells are shown as colored lines. Images

were captured at 15-min intervals. Scale bar, 20 μm.

9

Video S6. Effect of NOX2-knockdown on the directional movement of

surrounding cells toward RasV12-transformed cells, related to Figure 7

MDCK NOX2-shRNA1 cells were co-cultured with MDCK-pTR GFP-RasV12 cells

at a ratio of 50:1, followed by tetracycline treatment for 8 h, and then cell movement

of surrounding cells was observed by time-lapse imaging for 6 h. The trajectories of

the centroid of surrounding cells are shown as colored lines. Images were captured at

15-min intervals. Scale bar, 20 μm.

17

REFERENCES

1. Mitchell, S.J., and Rosenblatt, J. (2021). Early mechanical selection of cell extrusion and extrusion signaling in cancer. Curr Opin Cell Biol *72*, 36-40.
2. Villars, A., and Levayer, R. (2021). Collective effects in epithelial cell death and cell extrusion. Current opinion in genetics & development *72*, 8-14.
3. Gudipaty, S.A., and Rosenblatt, J. (2017). Epithelial cell extrusion: Pathways and pathologies. Semin Cell Dev Biol *67*, 132-140.
4. Ohsawa, S., Vaughen, J., and Igaki, T. (2018). Cell Extrusion: A Stress-Responsive Force for Good or Evil in Epithelial Homeostasis. Dev Cell *44*, 532.
5. Katoh, H., and Fujita, Y. (2012). Epithelial homeostasis: elimination by live cell extrusion. Curr Biol *22*, R453-455.
6. Amoyel, M., and Bach, E.A. (2014). Cell competition: how to eliminate your neighbours. Development *141*, 988-1000.
7. Johnston, L.A. (2009). Competitive interactions between cells: death, growth, and geography. Science *324*, 1679-1682.
8. Vishwakarma, M., and Piddini, E. (2020). Outcompeting cancer. Nat Rev Cancer *20*, 187-198.
9. Morata, G., and Calleja, M. (2020). Cell competition and tumorigenesis in the imaginal discs of Drosophila. Semin Cancer Biol *63*, 19-26.
10. Bowling, S., Lawlor, K., and Rodriguez, T.A. (2019). Cell competition: the winners and losers of fitness selection. Development *146*.
11. Diaz-Diaz, C., and Torres, M. (2019). Insights into the quantitative and dynamic aspects of Cell Competition. Curr Opin Cell Biol *60*, 68-74.
12. Madan, E., Gogna, R., and Moreno, E. (2018). Cell competition in development: information from flies and vertebrates. Curr Opin Cell Biol *55*, 150-157.
13. Maruyama, T., and Fujita, Y. (2017). Cell competition in mammals - novel homeostatic machinery for embryonic development and cancer prevention. Curr Opin Cell Biol *48*, 106-112.
14. Baker, N.E. (2020). Emerging mechanisms of cell competition. Nat Rev Genet *21*, 683-697.
15. Levayer, R. (2020). Solid stress, competition for space and cancer: The opposing roles of mechanical cell competition in tumour initiation and growth. Semin Cancer Biol *63*, 69-80.
16. Kajita, M., Sugimura, K., Ohoka, A., Burden, J., Suganuma, H., Ikegawa, M., Shimada, T., Kitamura, T., Shindoh, M., Ishikawa, S., et al. (2014). Filamin acts as a key regulator in epithelial defence against transformed cells. Nature communications *5*, 4428.
17. Kon, S., and Fujita, Y. (2021). Cell competition-induced apical elimination of transformed cells, EDAC, orchestrates the cellular homeostasis. Dev Biol *476*, 112-116.
18. Kajita, M., Hogan, C., Harris, A.R., Dupre-Crochet, S., Itasaki, N., Kawakami, K., Charras, G., Tada, M., and Fujita, Y. (2010). Interaction with surrounding normal epithelial cells influences signalling pathways and behaviour of Src-transformed cells. J Cell Sci *123*, 171-180.
19. Hogan, C., Dupre-Crochet, S., Norman, M., Kajita, M., Zimmermann, C., Pelling, A.E., Piddini, E., Baena-Lopez, L.A., Vincent, J.P., Itoh, Y., et al.

(2009). Characterization of the interface between normal and transformed epithelial cells. Nat Cell Biol *11*, 460-467.

20. Leung, C.T., and Brugge, J.S. (2012). Outgrowth of single oncogene-expressing cells from suppressive epithelial environments. Nature *482*, 410-413.

21. Norman, M., Wisniewska, K.A., Lawrenson, K., Garcia-Miranda, P., Tada, M., Kajita, M., Mano, H., Ishikawa, S., Ikegawa, M., Shimada, T., et al. (2012). Loss of Scribble causes cell competition in mammalian cells. J Cell Sci *125*, 59-66.

22. Brumby, A.M., and Richardson, H.E. (2003). scribble mutants cooperate with oncogenic Ras or Notch to cause neoplastic overgrowth in Drosophila. The EMBO journal *22*, 5769-5779.

23. Grzeschik, N.A., Amin, N., Secombe, J., Brumby, A.M., and Richardson, H.E. (2007). Abnormalities in cell proliferation and apico-basal cell polarity are separable in Drosophila lgl mutant clones in the developing eye. Dev Biol *311*, 106-123.

24. Igaki, T., Pagliarini, R.A., and Xu, T. (2006). Loss of cell polarity drives tumor growth and invasion through JNK activation in Drosophila. Curr Biol *16*, 1139-1146.

25. Rosenblatt, J., Raff, M.C., and Cramer, L.P. (2001). An epithelial cell destined for apoptosis signals its neighbors to extrude it by an actin- and myosin-dependent mechanism. Curr Biol *11*, 1847-1857.

26. Takeuchi, Y., Narumi, R., Akiyama, R., Vitiello, E., Shirai, T., Tanimura, N., Kuromiya, K., Ishikawa, S., Kajita, M., Tada, M., et al. (2020). Calcium Wave Promotes Cell Extrusion. Curr Biol *30*, 670-681 e676.

27. Duszyc, K., Gomez, G.A., Lagendijk, A.K., Yau, M.K., Nanavati, B.N., Gliddon, B.L., Hall, T.E., Verma, S., Hogan, B.M., Pitson, S.M., et al. (2021). Mechanotransduction activates RhoA in the neighbors of apoptotic epithelial cells to engage apical extrusion. Curr Biol *31*, 1326-1336 e1325.

28. Valon, L., Davidovic, A., Levillayer, F., Villars, A., Chouly, M., Cerqueira-Campos, F., and Levayer, R. (2021). Robustness of epithelial sealing is an emerging property of local ERK feedback driven by cell elimination. Dev Cell *56*, 1700-1711 e1708.

29. Gerasimovskaya, E.V., Ahmad, S., White, C.W., Jones, P.L., Carpenter, T.C., and Stenmark, K.R. (2002). Extracellular ATP is an autocrine/paracrine regulator of hypoxia-induced adventitial fibroblast growth. Signaling through extracellular signal-regulated kinase-1/2 and the Egr-1 transcription factor. The Journal of biological chemistry *277*, 44638-44650.

30. Elliott, M.R., Chekeni, F.B., Trampont, P.C., Lazarowski, E.R., Kadl, A., Walk, S.F., Park, D., Woodson, R.I., Ostankovich, M., Sharma, P., et al. (2009). Nucleotides released by apoptotic cells act as a find-me signal to promote phagocytic clearance. Nature *461*, 282-286.

31. Idzko, M., Ferrari, D., and Eltzschig, H.K. (2014). Nucleotide signalling during inflammation. Nature *509*, 310-317.

32. Faas, M.M., Saez, T., and de Vos, P. (2017). Extracellular ATP and adenosine: The Yin and Yang in immune responses? Mol Aspects Med *55*, 9-19.

33. Schwiebert, E.M., and Zsembery, A. (2003). Extracellular ATP as a signaling molecule for epithelial cells. Biochimica et biophysica acta *1615*, 7-32.

34. Hurd, T.R., DeGennaro, M., and Lehmann, R. (2012). Redox regulation of cell migration and adhesion. Trends Cell Biol *22*, 107-115.

35. Sies, H., and Jones, D.P. (2020). Reactive oxygen species (ROS) as pleiotropic physiological signalling agents. Nat Rev Mol Cell Biol *21*, 363-383.

36. Forrester, S.J., Kikuchi, D.S., Hernandes, M.S., Xu, Q., and Griendling, K.K. (2018). Reactive Oxygen Species in Metabolic and Inflammatory Signaling. Circ Res *122*, 877-902.

37. Kucinski, I., Dinan, M., Kolahgar, G., and Piddini, E. (2017). Chronic activation of JNK JAK/STAT and oxidative stress signalling causes the loser cell status. Nature communications *8*, 136.

38. Kon, S., Ishibashi, K., Katoh, H., Kitamoto, S., Shirai, T., Tanaka, S., Kajita, M., Ishikawa, S., Yamauchi, H., Yako, Y., et al. (2017). Cell competition with normal epithelial cells promotes apical extrusion of transformed cells through metabolic changes. Nat Cell Biol *19*, 530-541.

39. Dichmann, S., Idzko, M., Zimpfer, U., Hofmann, C., Ferrari, D., Luttmann, W., Virchow, C., Jr., Di Virgilio, F., and Norgauer, J. (2000). Adenosine triphosphate-induced oxygen radical production and CD11b up-regulation: Ca(++) mobilization and actin reorganization in human eosinophils. Blood *95*, 973-978.

40. Pines, A., Perrone, L., Bivi, N., Romanello, M., Damante, G., Gulisano, M., Kelley, M.R., Quadrifoglio, F., and Tell, G. (2005). Activation of APE1/Ref-1 is dependent on reactive oxygen species generated after purinergic receptor stimulation by ATP. Nucleic Acids Res *33*, 4379-4394.

41. Di Virgilio, F., Chiozzi, P., Ferrari, D., Falzoni, S., Sanz, J.M., Morelli, A., Torboli, M., Bolognesi, G., and Baricordi, O.R. (2001). Nucleotide receptors: an emerging family of regulatory molecules in blood cells. Blood *97*, 587-600.

42. Ralevic, V., and Burnstock, G. (1998). Receptors for purines and pyrimidines. Pharmacol Rev *50*, 413-492.

43. Sabirov, R.Z., and Okada, Y. (2005). ATP release via anion channels. Purinergic Signal *1*, 311-328.

44. Chekeni, F.B., Elliott, M.R., Sandilos, J.K., Walk, S.F., Kinchen, J.M., Lazarowski, E.R., Armstrong, A.J., Penuela, S., Laird, D.W., Salvesen, G.S., et al. (2010). Pannexin 1 channels mediate 'find-me' signal release and membrane permeability during apoptosis. Nature *467*, 863-867.

45. Diaz-Vegas, A., Campos, C.A., Contreras-Ferrat, A., Casas, M., Buvinic, S., Jaimovich, E., and Espinosa, A. (2015). ROS Production via P2Y1-PKC-NOX2 Is Triggered by Extracellular ATP after Electrical Stimulation of Skeletal Muscle Cells. PloS one *10*, e0129882.

46. Sudi, S.B., Tanaka, T., Oda, S., Nishiyama, K., Nishimura, A., Sunggip, C., Mangmool, S., Numaga-Tomita, T., and Nishida, M. (2019). TRPC3-Nox2 axis mediates nutritional deficiency-induced cardiomyocyte atrophy. Scientific reports *9*, 9785.

47. Cheng, S.E., Lee, I.T., Lin, C.C., Wu, W.L., Hsiao, L.D., and Yang, C.M. (2013). ATP mediates NADPH oxidase/ROS generation and COX-2/PGE2 expression in A549 cells: role of P2 receptor-dependent STAT3 activation. PloS one *8*, e54125.

48. Igaki, T., Pastor-Pareja, J.C., Aonuma, H., Miura, M., and Xu, T. (2009). Intrinsic tumor suppression and epithelial maintenance by endocytic activation of Eiger/TNF signaling in Drosophila. Dev Cell *16*, 458-465.

49. Rhiner, C., Lopez-Gay, J.M., Soldini, D., Casas-Tinto, S., Martin, F.A., Lombardia, L., and Moreno, E. (2010). Flower forms an extracellular code

that reveals the fitness of a cell to its neighbors in Drosophila. Dev Cell *18*, 985-998.

50. Yamamoto, M., Ohsawa, S., Kunimasa, K., and Igaki, T. (2017). The ligand Sas and its receptor PTP10D drive tumour-suppressive cell competition. Nature *542*, 246-250.

51. Meyer, S.N., Amoyel, M., Bergantinos, C., de la Cova, C., Schertel, C., Basler, K., and Johnston, L.A. (2014). An ancient defense system eliminates unfit cells from developing tissues during cell competition. Science *346*, 1258236.

52. Porazinski, S., de Navascues, J., Yako, Y., Hill, W., Jones, M.R., Maddison, R., Fujita, Y., and Hogan, C. (2016). EphA2 Drives the Segregation of Ras-Transformed Epithelial Cells from Normal Neighbors. Curr Biol *26*, 3220-3229.

53. Portela, M., Casas-Tinto, S., Rhiner, C., Lopez-Gay, J.M., Dominguez, O., Soldini, D., and Moreno, E. (2010). Drosophila SPARC is a self-protective signal expressed by loser cells during cell competition. Dev Cell *19*, 562-573.

54. Ogawa, M., Kawarazaki, Y., Fujita, Y., Naguro, I., and Ichijo, H. (2021). FGF21 Induced by the ASK1-p38 Pathway Promotes Mechanical Cell Competition by Attracting Cells. Curr Biol *31*, 1048-1057 e1045.

55. Gu, Y., Forostyan, T., Sabbadini, R., and Rosenblatt, J. (2011). Epithelial cell extrusion requires the sphingosine-1-phosphate receptor 2 pathway. J Cell Biol *193*, 667-676.

56. Kouzaki, H., Iijima, K., Kobayashi, T., O'Grady, S.M., and Kita, H. (2011). The danger signal, extracellular ATP, is a sensor for an airborne allergen and triggers IL-33 release and innate Th2-type responses. J Immunol *186*, 4375-4387.

57. Saez, P.J., Vargas, P., Shoji, K.F., Harcha, P.A., Lennon-Dumenil, A.M., and Saez, J.C. (2017). ATP promotes the fast migration of dendritic cells through the activity of pannexin 1 channels and P2X7 receptors. Sci Signal *10*.

58. Idzko, M., Hammad, H., van Nimwegen, M., Kool, M., Willart, M.A., Muskens, F., Hoogsteden, H.C., Luttmann, W., Ferrari, D., Di Virgilio, F., et al. (2007). Extracellular ATP triggers and maintains asthmatic airway inflammation by activating dendritic cells. Nat Med *13*, 913-919.

59. Sabirov, R.Z., Merzlyak, P.G., Okada, T., Islam, M.R., Uramoto, H., Mori, T., Makino, Y., Matsuura, H., Xie, Y., and Okada, Y. (2017). The organic anion transporter SLCO2A1 constitutes the core component of the Maxi-Cl channel. The EMBO journal *36*, 3309-3324.

60. Liu, H.T., Tashmukhamedov, B.A., Inoue, H., Okada, Y., and Sabirov, R.Z. (2006). Roles of two types of anion channels in glutamate release from mouse astrocytes under ischemic or osmotic stress. Glia *54*, 343-357.

61. Liu, H.T., Toychiev, A.H., Takahashi, N., Sabirov, R.Z., and Okada, Y. (2008). Maxi-anion channel as a candidate pathway for osmosensitive ATP release from mouse astrocytes in primary culture. Cell Res *18*, 558-565.

62. Liu, H.T., Sabirov, R.Z., and Okada, Y. (2008). Oxygen-glucose deprivation induces ATP release via maxi-anion channels in astrocytes. Purinergic Signal *4*, 147-154.

63. Sabirov, R.Z., and Okada, Y. (2009). The maxi-anion channel: a classical channel playing novel roles through an unidentified molecular entity. J Physiol Sci *59*, 3-21.

64. Ushio-Fukai, M. (2006). Localizing NADPH oxidase-derived ROS. Sci STKE *2006*, re8.

65. Moldovan, L., Moldovan, N.I., Sohn, R.H., Parikh, S.A., and Goldschmidt-Clermont, P.J. (2000). Redox changes of cultured endothelial cells and actin dynamics. Circ Res *86*, 549-557.

66. Wu, R.F., Gu, Y., Xu, Y.C., Nwariaku, F.E., and Terada, L.S. (2003). Vascular endothelial growth factor causes translocation of p47phox to membrane ruffles through WAVE1. The Journal of biological chemistry *278*, 36830-36840.

67. Aikin, T.J., Peterson, A.F., Pokrass, M.J., Clark, H.R., and Regot, S. (2020). MAPK activity dynamics regulate non-cell autonomous effects of oncogene expression. eLife *9*.

68. Liu, N., Matsumura, H., Kato, T., Ichinose, S., Takada, A., Namiki, T., Asakawa, K., Morinaga, H., Mohri, Y., De Arcangelis, A., et al. (2019). Stem cell competition orchestrates skin homeostasis and ageing. Nature *568*, 344-350.

69. Bastounis, E.E., Serrano-Alcalde, F., Radhakrishnan, P., Engstrom, P., Gomez-Benito, M.J., Oswald, M.S., Yeh, Y.T., Smith, J.G., Welch, M.D., Garcia-Aznar, J.M., et al. (2021). Mechanical competition triggered by innate immune signaling drives the collective extrusion of bacterially infected epithelial cells. Dev Cell *56*, 443-460 e411.

70. Akieda, Y., Ogamino, S., Furuie, H., Ishitani, S., Akiyoshi, R., Nogami, J., Masuda, T., Shimizu, N., Ohkawa, Y., and Ishitani, T. (2019). Cell competition corrects noisy Wnt morphogen gradients to achieve robust patterning in the zebrafish embryo. Nature communications *10*, 4710.

71. Hashimoto, M., and Sasaki, H. (2019). Epiblast Formation by TEAD-YAP-Dependent Expression of Pluripotency Factors and Competitive Elimination of Unspecified Cells. Dev Cell *50*, 139-154 e135.

72. Merino, M.M., Rhiner, C., Lopez-Gay, J.M., Buechel, D., Hauert, B., and Moreno, E. (2015). Elimination of unfit cells maintains tissue health and prolongs lifespan. Cell *160*, 461-476.

73. Ohoka, A., Kajita, M., Ikenouchi, J., Yako, Y., Kitamoto, S., Kon, S., Ikegawa, M., Shimada, T., Ishikawa, S., and Fujita, Y. (2015). EPLIN is a crucial regulator for extrusion of RasV12-transformed cells. J Cell Sci *128*, 781-789.

74. Hogan, C., Serpente, N., Cogram, P., Hosking, C.R., Bialucha, C.U., Feller, S.M., Braga, V.M., Birchmeier, W., and Fujita, Y. (2004). Rap1 regulates the formation of E-cadherin-based cell-cell contacts. Mol Cell Biol *24*, 6690-6700.

Figure 1

A

	MDCK alone	MDCK GFP-RasV12 alone	MDCK :RasV12=50:1
RasV12			
CellROX			

B

□ Single culture
■ MDCK:RasV12=50:1

CellROX intensity

NS
**
*

+ tet 16 h

MDCK | RasV12 | RasV12 | MDCK

MDCK:
RasV12=50:1

C

MDCK:RasV12=50:1

	DMSO	Trolox
RasV12		
CellROX		

D

□ Single culture
■ MDCK:RasV12=50:1

CellROX intensity

*
*

MDCK | RasV12 | RasV12 | MDCK | RasV12 | MDCK

DMSO | Trolox

E

MDCK:RasV12=50:1

DMSO
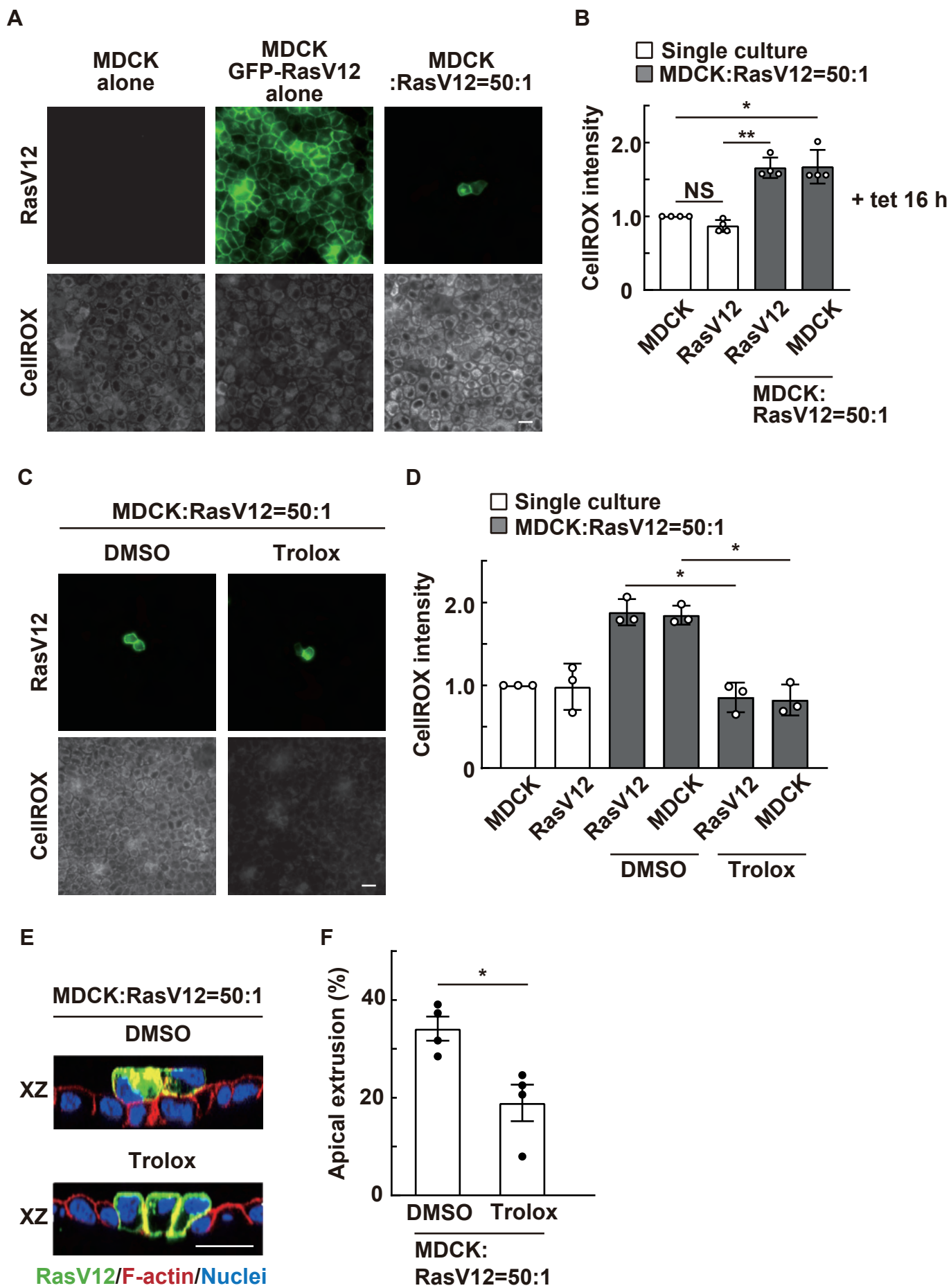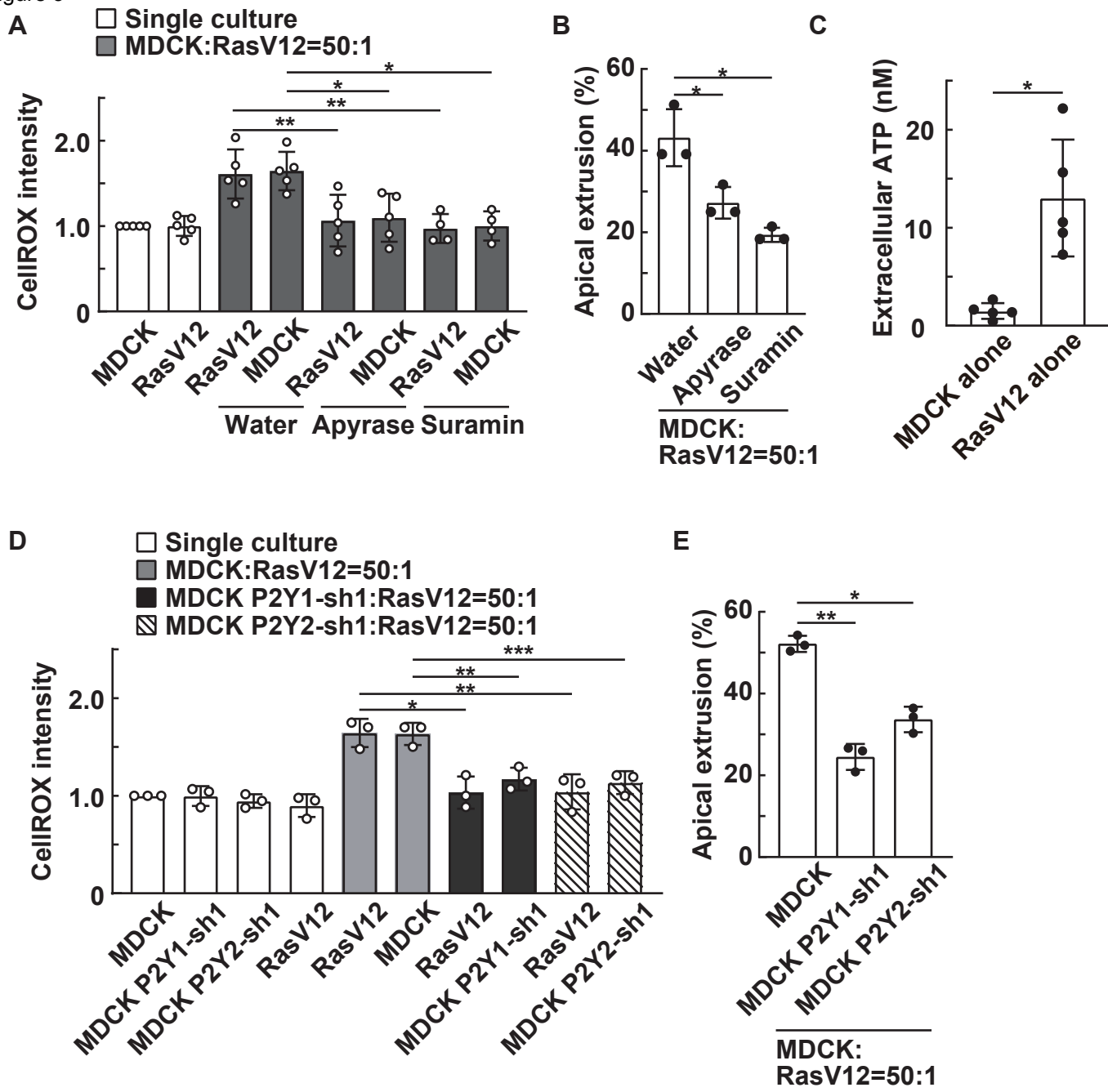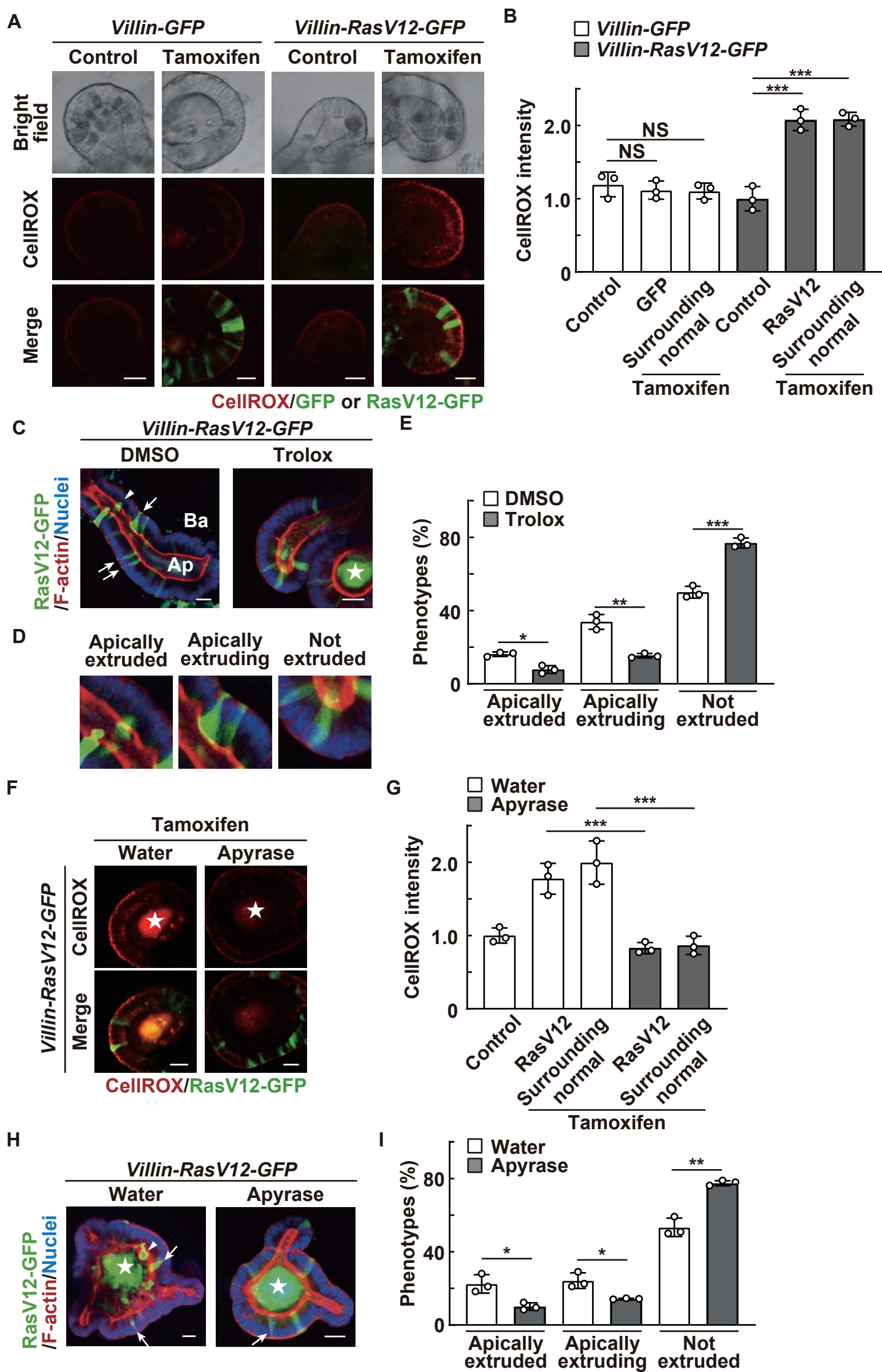XZ

Trolox
XZ

RasV12/F-actin/Nuclei

F

Apical extrusion (%)

*

DMSO | Trolox

MDCK:
RasV12=50:1

Figure 2

Figure 3

Figure 4

A

| | *Villin-GFP* | | *Villin-RasV12-GFP* | |
| | Control | Tamoxifen | Control | Tamoxifen |

Bright field

CellROX

Merge

CellROX/GFP or RasV12-GFP

B

□ *Villin-GFP*
■ *Villin-RasV12-GFP*

CellROX intensity

NS   NS   ***   ***

Control GFP Surrounding normal Control RasV12 Surrounding normal

Tamoxifen   Tamoxifen

C *Villin-RasV12-GFP*

DMSO   Trolox

RasV12-GFP/F-actin/Nuclei

Ba   Ap

D

Apically extruded   Apically extruding   Not extruded

E

□ DMSO
■ Trolox

Phenotypes (%)

*   **   ***

Apically extruded   Apically extruding   Not extruded

F   Tamoxifen

Water   Apyrase

Villin-RasV12-GFP

CellROX

Merge

CellROX/RasV12-GFP

G

□ Water
■ Apyrase

CellROX intensity

***   ***

Control RasV12 Surrounding normal RasV12 Surrounding normal

Tamoxifen

H *Villin-RasV12-GFP*

Water   Apyrase

RasV12-GFP/F-actin/Nuclei

I

□ Water
■ Apyrase

Phenotypes (%)

*   *   **

Apically extruded   Apically extruding   Not extruded

Figure 5

A

MDCK alone | MDCK Scrib-shRNA alone | MDCK :Scrib=10:1

Scrib

CellROX

B

□ Single culture
■ MDCK:Scrib=10:1

CellROX intensity

MDCK | Scrib | Scrib | MDCK

MDCK:Scrib=10:1

NS * *

C

MDCK:Scrib=10:1

DMSO | Trolox

Scrib

CellROX

D

□ Single culture
■ MDCK:Scrib=10:1

CellROX intensity

MDCK | Scrib | Scrib | MDCK | Scrib | MDCK

DMSO | Trolox

**

E

Extrusion of Scrib cells (%)

DMSO | Trolox

MDCK:Scrib =10:1

*

F

Extracellular ATP (nM)

MDCK alone | Scrib alone

*

G

□ Single culture
■ MDCK:Scrib=10:1
■ MDCK P2Y1-sh1:Scrib=10:1
▨ MDCK P2Y2-sh1:Scrib=10:1

CellROX intensity

MDCK | MDCK P2Y1-sh1 | MDCK P2Y2-sh1 | Scrib | Scrib | MDCK | Scrib | MDCK P2Y1-sh1 | Scrib | MDCK P2Y2-sh1

** ** **

H

Extrusion of Scrib cells (%)

MDCK | MDCK P2Y1-sh1 | MDCK P2Y2-sh1

MDCK:Scrib =10:1

** *

Figure 6

A

MDCK-pTR
GFP-Caspase-8
+ tet

(kDa)   MDCK   0   3   4   5   (h)

GFP 63

Cleaved
Caspase-3   28
17

Actin 48

B

MDCK:Casp-8=50:1

XZ

Cleaved-caspase-3/
caspase-8/Nuclei/F-actin

C

Extracellular ATP (nM)

MDCK alone   Casp-8 alone

D

MDCK
alone

MDCK
GFP-Caspase-8
alone

MDCK
:Casp-8=50:1

Caspase-8

CellROX

E

☐ Single culture
■ MDCK:Casp-8=50:1

CellROX intensity

MDCK   Casp-8   Casp-8   MDCK

MDCK:
Casp-8=50:1

F

MDCK:Casp-8=50:1

Water   Apyrase

Caspase-8

CellROX

G

☐ Single culture
■ MDCK:Casp-8=50:1

CellROX intensity

MDCK   Casp-8   Casp-8   MDCK   Casp-8   MDCK

Water   Apyrase

H

MDCK:Casp-8=50:1

DMSO   Trolox   Z-VAD-FMK

Caspase-8

CellROX

I

☐ Single culture
■ MDCK:Caspase-8=50:1

CellROX intensity

MDCK   Casp-8   Casp-8   MDCK   Casp-8   MDCK   Casp-8   MDCK

DMSO   Trolox   Z-VAD-FMK

J

Extrusion time (min)

Water   Apyrase   DMSO   Trolox

MDCK:Casp-8=50:1

Figure 7

A

Extruding cell
Centroid
Cell$_{t1}$
θ
Cell$_{t0}$

Arrow length = Distance
Angle (θ) = Direction

B

Distance of cell migration (μm)

MDCK alone
MDCK NOX2-sh1 alone
MDCK
MDCK with Trolox
MDCK NOX2-sh1

MDCK:RasV12 =50:1

C

☐ MDCK ▨ MDCK with Trolox
■ MDCK NOX2-sh1

Percentage

0-45   45-90   90-135   135-180
Angle (θ)

D

Distance of cell migration (μm)

MDCK alone
MDCK P2Y1-sh1 alone
MDCK P2Y2-sh1 alone
MDCK
MDCK with Apyrase
MDCK P2Y1-sh1
MDCK P2Y2-sh1

MDCK:RasV12 =50:1

E

☐ MDCK ▨ MDCK with Apyrase
■ MDCK P2Y1-sh1 ▨ MDCK P2Y2-sh1

Percentage

0-45   45-90   90-135   135-180
Angle (θ)

F

Distance of cell migration (μm)

MDCK alone
MDCK (Water)
MDCK with Apyrase
MDCK (DMSO)
MDCK with Trolox

MDCK:Casp-8=50:1

G

☐ MDCK (Water) ▨ MDCK with Apyrase
■ MDCK (DMSO) ▨ MDCK with Trolox

Percentage

0-45   45-90   90-135   135-180
Angle (θ)

H

Extracellular ATP↑

Transformed or Apoptotic cell

Release

ROS↑
Migration↑

Extrusion

Normal cell

A

B MDCK:RasV12 co-culture

C

D

E

F

G

H

Figure S1. ROS promote apical extrusion of SrcY527F-transformed cells from the epithelial layer, related to Figure 1

(A) The intracellular ROS level in the single- or co-cultured normal and RasV12-transformed cells. Normal MDCK cells and MDCK-pTR GFP-RasV12 cells were cultured alone or co-cultured at a ratio of 50:1, followed by the treatment with tetracycline for 8, 10, 12, or 24 h, and the intracellular ROS level was examined by CellROX. Values are expressed as a ratio relative to single-cultured MDCK cells at each time point. Data are mean ± SD from three independent experiments. *$p < 0.05$ and NS: not significant (paired two-tailed Student's t-test); n = 180, 180, 117, 293, 180, 180, 180, 310, 180, 180, 156, 352, 180, 180, 121, and 341 cells.

(B) Intracellular ROS level in the single- or co-cultured normal and RasV12-transformed cells at various mixing ratios. Normal MDCK cells and MDCK-pTR GFP-RasV12 cells were cultured alone or co-cultured at a ratio of 1:1, 10:1, 50:1, 100:1, or 2,000:1, followed by the treatment with tetracycline for 16 h, and the intracellular ROS level was examined by CellROX.

(C) Quantification of fluorescent intensity of CellROX in the surrounding normal cells within 160 μm from RasV12-transformed cells. MDCK cells were cultured alone or co-cultured with MDCK-pTR GFP-RasV12 cells at a ratio of 2,000:1, followed by CellROX analysis. For MDCK cells cultured alone, CellROX fluorescent intensity was measured within 160 μm from randomly selected cells. Values are expressed as a ratio relative to MDCK cells alone at 0 μm. Three representative results are shown for cells that show evenly distributed (left) or gradually decreased CellROX intensity around RasV12 cells (right).

(D and E) The intracellular ROS level in single- or co-cultured normal and GFP-expressing cells. Normal MDCK and MDCK-pTR GFP cells were cultured alone or co-cultured at a ratio of 50:1, followed by CellROX analysis. (D) CellROX fluorescent images. (E) Quantification of fluorescent intensity of CellROX. Values are expressed as a ratio relative to single-cultured MDCK cells. Data are mean ± SD from three independent experiments. NS: not significant (one-way ANOVA with Tukey's test); n = 166, 166, 162, and 126 cells.

(F and G) The intracellular ROS level in single- or co-cultured normal and SrcY527F-transformed cells. Normal MDCK cells and MDCK-pTR GFP-SrcY527F cells were cultured alone or co-cultured at a ratio of 50:1, followed by CellROX analysis. (F) CellROX fluorescent images. (G) Quantification of fluorescent intensity of CellROX. Values are expressed as a ratio relative to single-cultured MDCK cells. Data are mean ± SD from four independent experiments. *p < 0.05, ** p< 0.01, and NS: not significant (one-way ANOVA with Tukey's test); n = 240, 240, 130, and 360 cells.

(H) Effect of Trolox on apical extrusion of SrcY527F-transformed cells surrounded by normal cells. Data are mean ± SD from three independent experiments. *p < 0.05 (paired two-tailed Student's t-test); n = 292 and 293 cells.
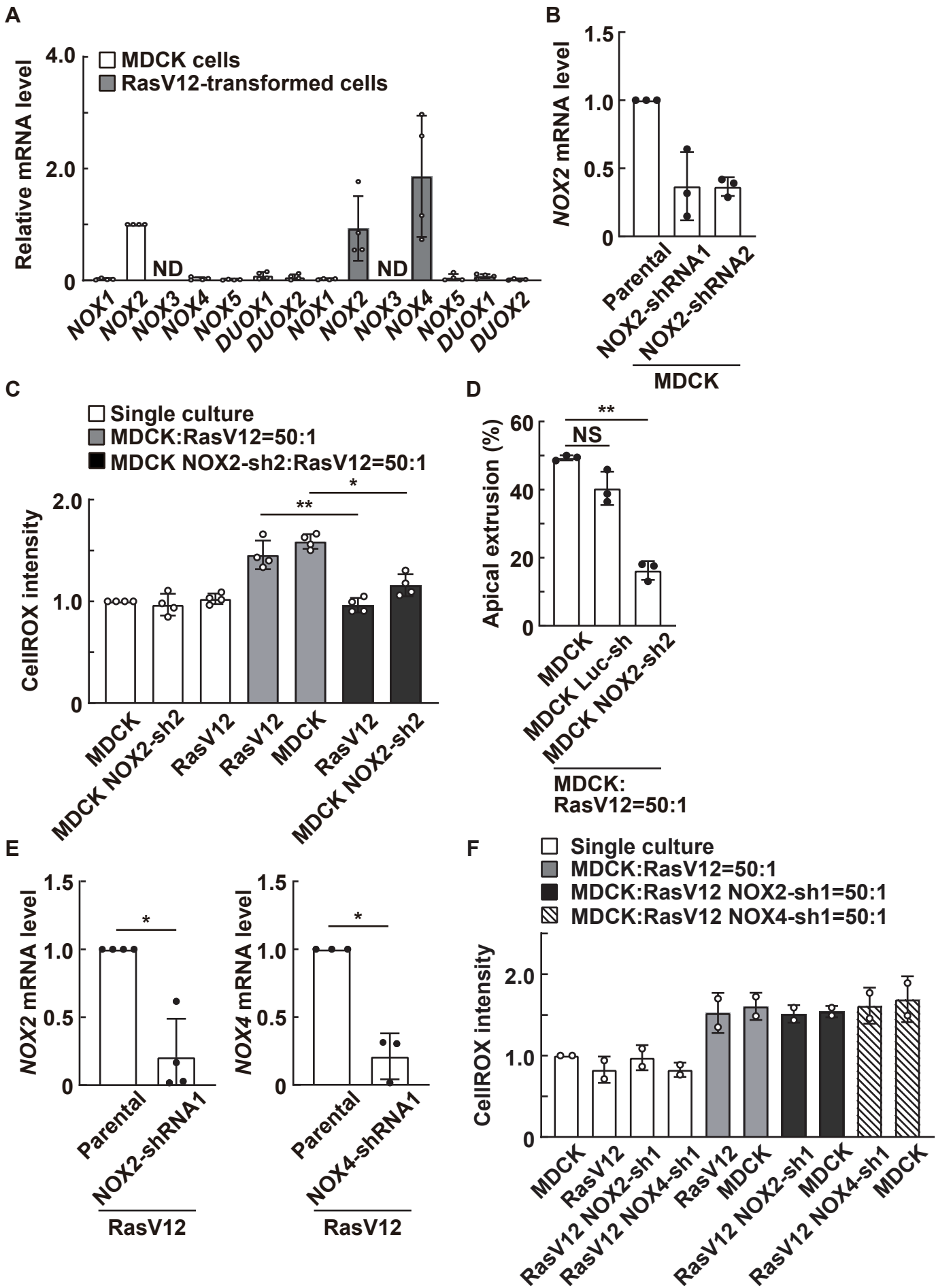
(B, D, and F) Scale bars, 20 μm.

Figure S2. NOX2 in surrounding normal cells promotes apical extrusion of RasV12-transformed cells, related to Figure 2

(A) Quantitative real-time PCR analysis of NADPH oxidases in normal cells or RasV12-transformed cells cultured alone. Values are expressed as a ratio relative to *NOX2* expression in MDCK cells. Data are mean ± SD from four independent experiments. ND: not detected.

(B) Effect of NOX2-shRNA expression on the *NOX2* mRNA level in MDCK cells. Values are expressed as a ratio relative to parental MDCK cells. Data are mean ± SD from three independent experiments.

(C and D) Effect of NOX2-knockdown in surrounding cells on the intracellular ROS level (C) and apical extrusion (D). (C) Quantification of fluorescent intensity of CellROX. MDCK-pTR GFP-RasV12 cells were cultured alone or co-cultured with normal MDCK or MDCK NOX2-shRNA2 cells at a ratio of 1:50, followed by CellROX analysis. Values are expressed as a ratio relative to single-cultured MDCK cells. Data are mean ± SD from four independent experiments. *$p < 0.05$ and **$p < 0.01$ (one-way ANOVA with Dunnett's test); n = 240, 240, 240, 266, 638, 190, and 448 cells.

(D) Effect of NOX2-knockdown in surrounding cells on apical extrusion of RasV12-transformed cells. Data are mean ± SD from three independent experiments. **$p < 0.01$ and NS: not significant (one-way ANOVA with Dunnett's test); n = 362, 324, and 409 cells.

(E) Effect of NOX2-shRNA or NOX4-shRNA expression on the *NOX2* or *NOX4* mRNA level in MDCK-pTR GFP-RasV12 cells respectively. Data are mean ± SD from three (for NOX4) or four (for NOX2) independent experiments. *$p < 0.05$ (paired two-tailed Student's t-test).

(F) Effect of NOX2-knockdown or NOX4-knockdown in RasV12-transformed cells on the intracellular ROS level. MDCK-pTR GFP-RasV12, MDCK-pTR GFP-RasV12 NOX2-shRNA1, or MDCK-pTR GFP-RasV12 NOX4-shRNA1 cells were cultured alone or co-cultured with normal MDCK cells at a ratio of 1:50, followed by CellROX analysis. Values are expressed as a ratio relative to single-cultured MDCK cells. Data are mean ± SD from two independent experiments; n = 120, 120, 120, 120, 94, 262, 94, 199, 70, and 100 cells.
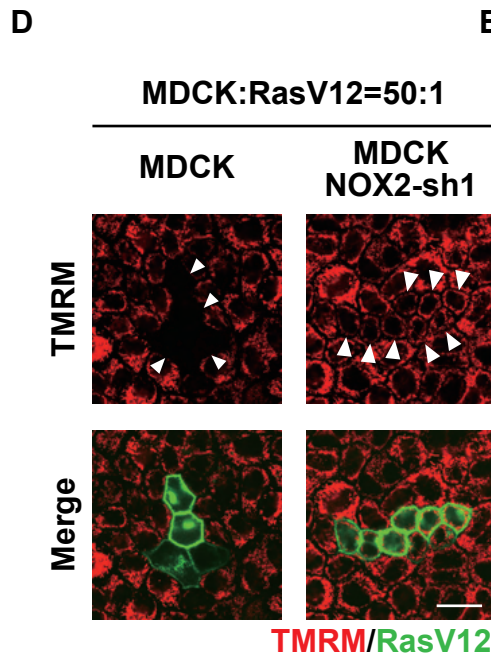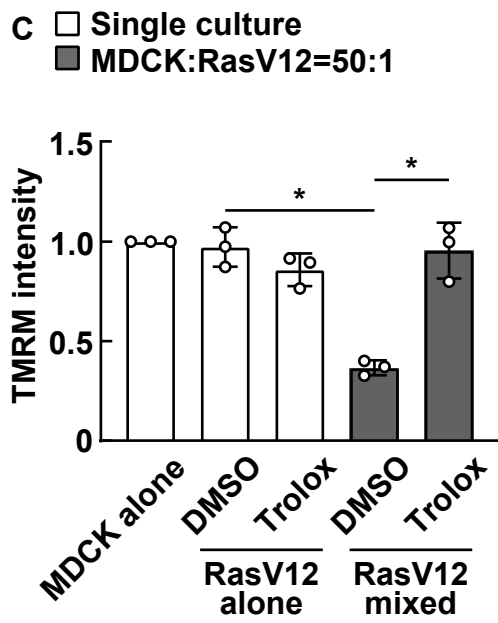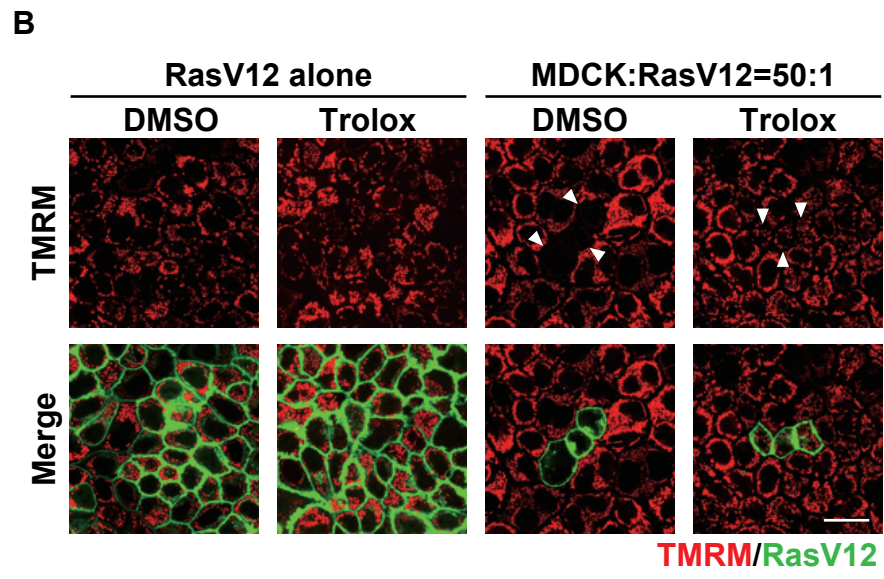
A ☐ Single culture ☐ MDCK:RasV12=50:1

PDK4 mRNA level

NS

B RasV12 alone | MDCK:RasV12=50:1

DMSO | Trolox | DMSO | Trolox

TMRM

Merge

TMRM/RasV12

C ☐ Single culture ☐ MDCK:RasV12=50:1

TMRM intensity

MDCK alone | DMSO | Trolox | DMSO | Trolox

RasV12 alone | RasV12 mixed

D MDCK:RasV12=50:1

MDCK | MDCK NOX2-sh1

TMRM

Merge

TMRM/RasV12

E ☐ Single culture ☐ MDCK:RasV12=50:1

TMRM intensity

MDCK alone | RasV12 alone | RasV12 with MDCK | RasV12 with MDCK NOX2-sh1

Figure S3. ROS induce the decreased mitochondrial membrane potential in RasV12-transformed cells surrounded by normal cells, related to Figure 2

(A) Effect of NOX2-knockdown in surrounding cells on the *PDK4* mRNA level in RasV12-transformed cells. MDCK-pTR GFP-RasV12 cells were cultured alone or co-cultured with normal MDCK or MDCK NOX2-shRNA cells at a ratio of 1:10. GFP-positive RasV12 cells were selectively collected by FACS sorting and subjected to qPCR analysis. Values are expressed as a ratio relative to RasV12 cells cultured alone. Data are mean ± SD from three independent experiments. *p < 0.05 and NS: not significant (one-way ANOVA with Dunnett's test).

(B and C) Effect of Trolox on the TMRM incorporation in RasV12-transformed cells surrounded by normal cells. MDCK-pTR GFP-RasV12 cells were cultured alone or co-cultured with normal MDCK cells at a ratio of 1:50 in the absence or presence of Trolox, followed by loading with TMRM. (B) TMRM fluorescent images. Arrowheads indicate RasV12 cells surrounded by normal cells. (C) Quantification of fluorescent intensity of TMRM. Values are expressed as a ratio relative to single-cultured MDCK cells. Data are mean ± SD from three independent experiments. *p < 0.05 (one-way ANOVA with Dunnett's test); n = 240, 240, 240, 285, and 210 cells.

(D and E) Effect of NOX2-knockdown in surrounding cells on the TMRM incorporation in RasV12-transformed cells. MDCK-pTR GFP-RasV12 cells were co-cultured with normal MDCK or MDCK NOX2-shRNA1 cells at a ratio of 1:50, followed by loading with TMRM. (D) TMRM fluorescent images. Arrowheads indicate RasV12 cells. (E) Quantification of fluorescent intensity of TMRM. Values are expressed as a ratio relative to single-cultured MDCK cells. Data are mean ± SD from

three independent experiments. *p < 0.05 (one-way ANOVA with Dunnett's test); n =

180, 180, 199, and 353 cells.
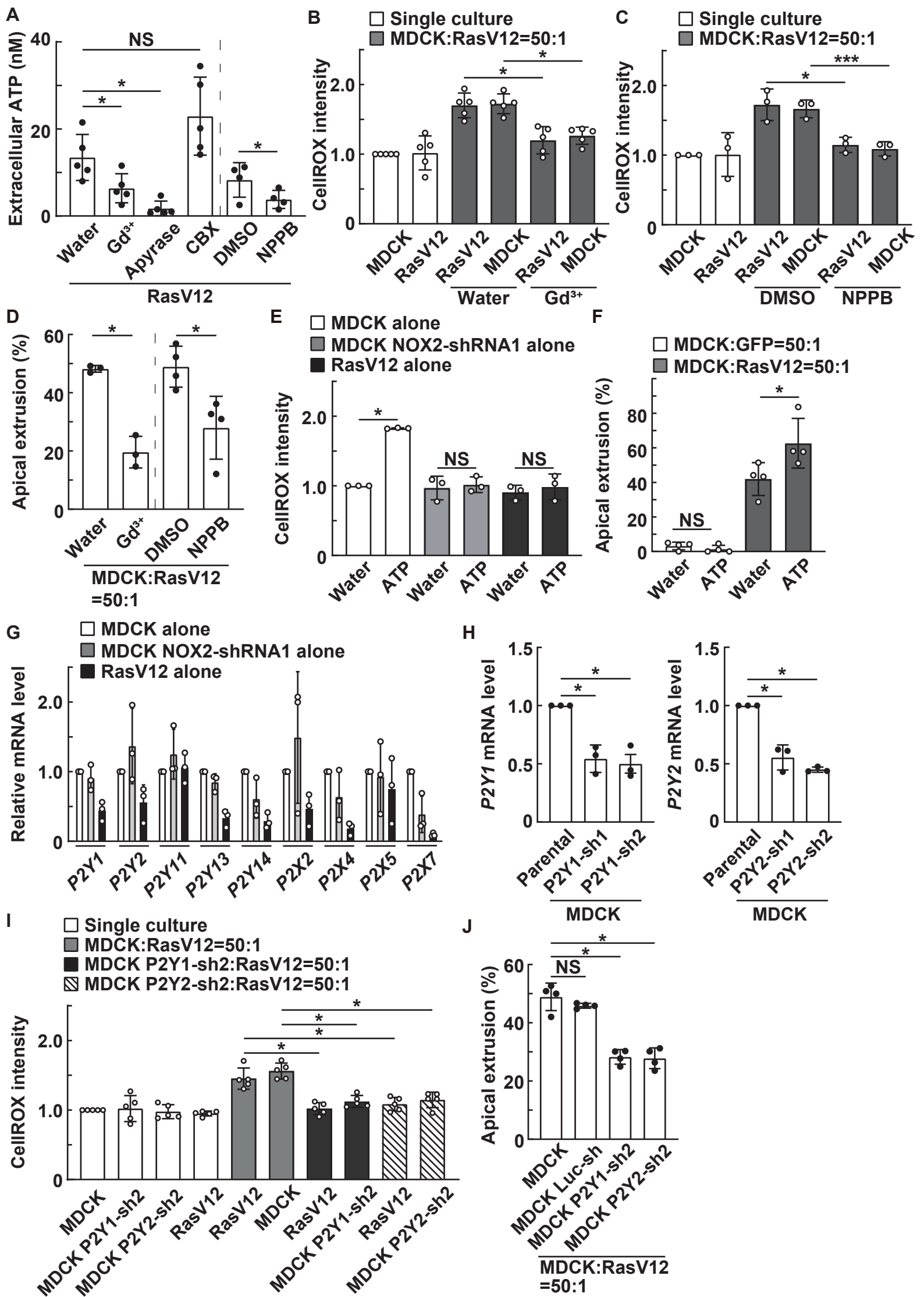
(B and D) Scale bars, 20 μm.

Figure S4. Extracellular ATP signal via P2Y1 or P2Y2 receptor in surrounding cells promotes apical extrusion of RasV12-transformed cells, related to Figure 3

(A) Effect of an inhibitor for ATP release channel on the extracellular ATP level of RasV12-transformed cells. MDCK-pTR GFP-Rasv12 cells were treated with Gd^{3+}, apyrase, CBX, or NPPB, and the extracellular ATP level in conditioned media was measured using CellTiter-Glo 2.0 reagent. Data are mean ± SD from four (right two) or five (left four) independent experiments. *p<0.05 and NS: not significant (paired two-tailed Student's t-test (right two) or one-way ANOVA with Dunnett's test (left four)).

(B-D) Effect of Gd^{3+} or NPPB treatment on the intracellular ROS level (B and C) or apical extrusion (D). (B and C) Quantification of fluorescent intensity of CellROX. Normal MDCK and MDCK-pTR GFP-RasV12 cells were cultured alone or co-cultured in the absence or presence of Gd^{3+} (B) or NPPB (C), followed by CellROX analysis. Values are expressed as a ratio relative to single-cultured MDCK cells. Data are mean ± SD from five (B) or three (C) independent experiments. *p < 0.05 and ***p < 0.001 (one-way ANOVA with Dunnett's test); n = 299, 300, 266, 657, 217, and 473 cells (B) or 179, 185, 139, 312, 86, and 274 cells (C). (D) Effect of Gd^{3+} or NPPB treatment on apical extrusion of RasV12-transformed cells. Data are mean ± SD from three (Water- or Gd^{3+}-treated cells) or four (DMSO- or NPPB-treated cells) independent experiments. *p < 0.05 (paired two-tailed Student's t-test); n = 355, 400, 499, and 346 cells.

(E and F) Effect of exogenous ATP treatment on the intracellular ROS level (E) or apical extrusion (F). (E) Quantification of fluorescent intensity of CellROX. Normal MDCK, MDCK NOX2-shRNA1, or MDCK-pTR GFP-RasV12 cells were cultured alone in the absence or presence of exogenous ATP for 30 min, followed by CellROX analysis. Values are expressed as a ratio relative to water-treated MDCK cells. Data are

mean ± SD from three independent experiments. *p < 0.05 and NS: not significant (paired two-tailed Student's t-test); n = 180 cells for all conditions. (F) Quantification of apical extrusion of RasV12 cells. MDCK-pTR GFP or MDCK-pTR GFP-RasV12 cells were co-cultured with normal MDCK cells at a ratio of 1:50 in the absence or presence of exogenous ATP for 24 h. Data are mean ± SD from four independent experiments. *p < 0.05 and NS: not significant (paired two-tailed Student's t-test); n = 358, 402, 400, and 356 cells.
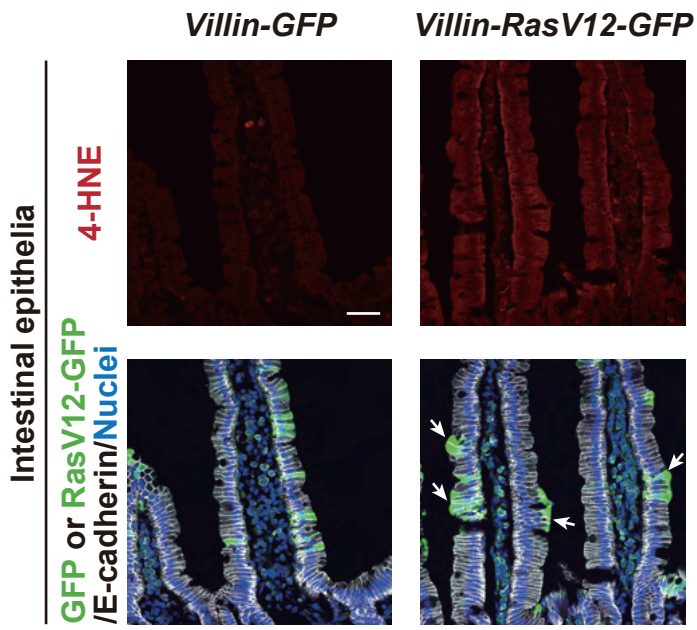
(G) Quantitative real-time PCR analysis of the P2Y or P2X receptors in normal MDCK, MDCK NOX2-shRNA1, or MDCK-pTR GFP-RasV12 cells. Values are expressed as a ratio relative to MDCK cells. Data are mean ± SD from three independent experiments. Note that the expression of *P2Y4*, *P2Y6*, *P2Y12*, *P2X1*, *P2X3*, or *P2X6* was not detected in this qPCR analysis.

(H) Effect of P2Y1-shRNA or P2Y2-shRNA expression on the *P2Y1* or *P2Y2* mRNA level in MDCK cells. Data are mean ± SD from three independent experiments. *p < 0.05 (one-way ANOVA with Dunnett's test).
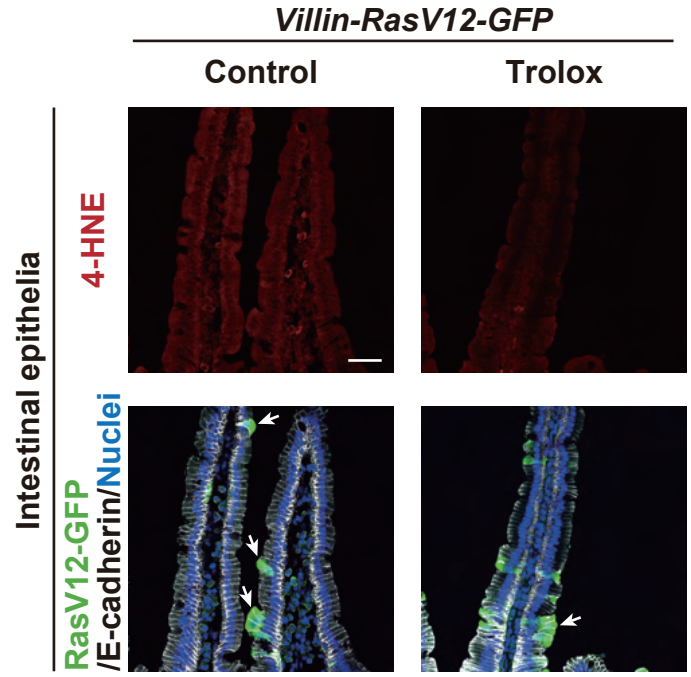
(I and J) Effect of P2Y1- or P2Y2-knockdown in surrounding cells on the intracellular ROS level (I) or apical extrusion (J). (I) Quantification of fluorescent intensity of CellROX. MDCK-pTR GFP-RasV12 cells were cultured alone or co-cultured with normal MDCK, MDCK P2Y1-shRNA2, or MDCK P2Y2-shRNA2 cells, followed by CellROX analysis. Values are expressed as a ratio relative to single-cultured MDCK cells. Data are mean ± SD from five independent experiments. *p < 0.05 (one-way ANOVA with Dunnett's test); n = 300, 300, 300, 300, 217, 427, 234, 460, 180, and 325 cells. (J) Effect of P2Y1- or P2Y2-knockdown in surrounding cells on apical extrusion of RasV12-transformed cells. Data are mean ± SD from four independent experiments.

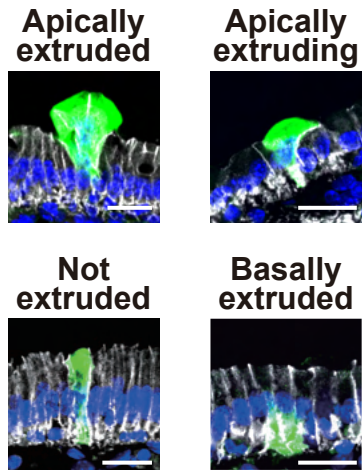*p < 0.05 and NS: not significant (one-way ANOVA with Dunnett's test); n = 424, 525, 528, and 550 cells.

A

Villin-GFP   *Villin-RasV12-GFP*

Intestinal epithelia

4-HNE

GFP or RasV12-GFP /E-cadherin/Nuclei

B

Villin-RasV12-GFP

Control   Trolox

Intestinal epithelia

4-HNE

RasV12-GFP /E-cadherin/Nuclei

C

Apically extruded

Apically extruding

Not extruded

Basally extruded

D

□ Control
■ Trolox

Phenotypes (%)

*** NS *** NS

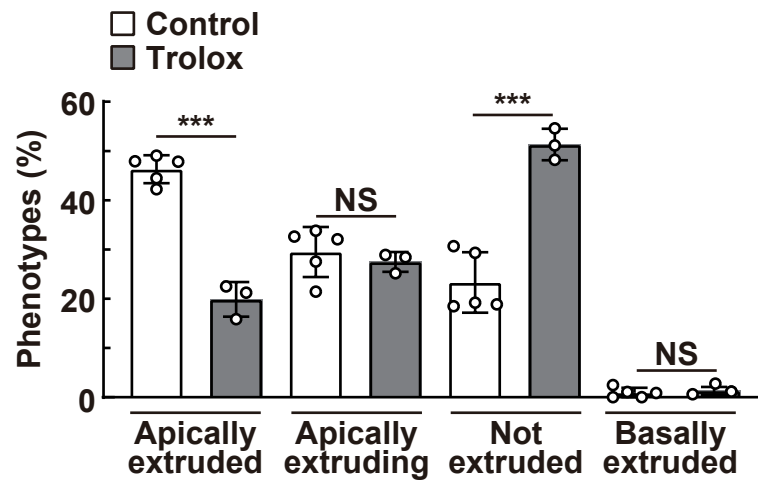Apically extruded   Apically extruding   Not extruded   Basally extruded

Figure S5. Oxidative stress promotes apical extrusion of RasV12-transformed cells from mouse intestinal epithelia, related to Figure 4

(A and B) Immunofluorescent analysis for 4-HNE in intestinal epithelia from *villin-Cre^{ERT2}-LSL-eGFP* or *-LSL-Ras^{V12}-IRES-eGFP* mice at 3 days after tamoxifen administration with or without Trolox treatment. The arrows indicate apically extruded or extruding RasV12-expressing cells.

(C) Classification of the phenotypes of RasV12-expressing cells in intestinal epithelia of *villin-Cre^{ERT2}-LSL-Ras^{V12}-IRES-eGFP* mice. 'apically extruded': completely detached from the basement membrane and translocated into the apical lumen. 'apically extruding': with their nucleus apically shifted, but still attached to the basement membrane. 'not extruded': remaining within the epithelium. 'Basally extruded': basally delaminated from the epithelial layer.

(D) Quantification of the phenotypes of RasV12-expressing cells in intestinal epithelia at 3 days after tamoxifen administration with or without Trolox treatment. Data are mean ± SD from three independent experiments. ***$p < 0.001$ and NS: not significant (unpaired two-tailed Student's t-test); n = 1,258 or 855 cells from five (Control) or three (Trolox) mice, respectively.

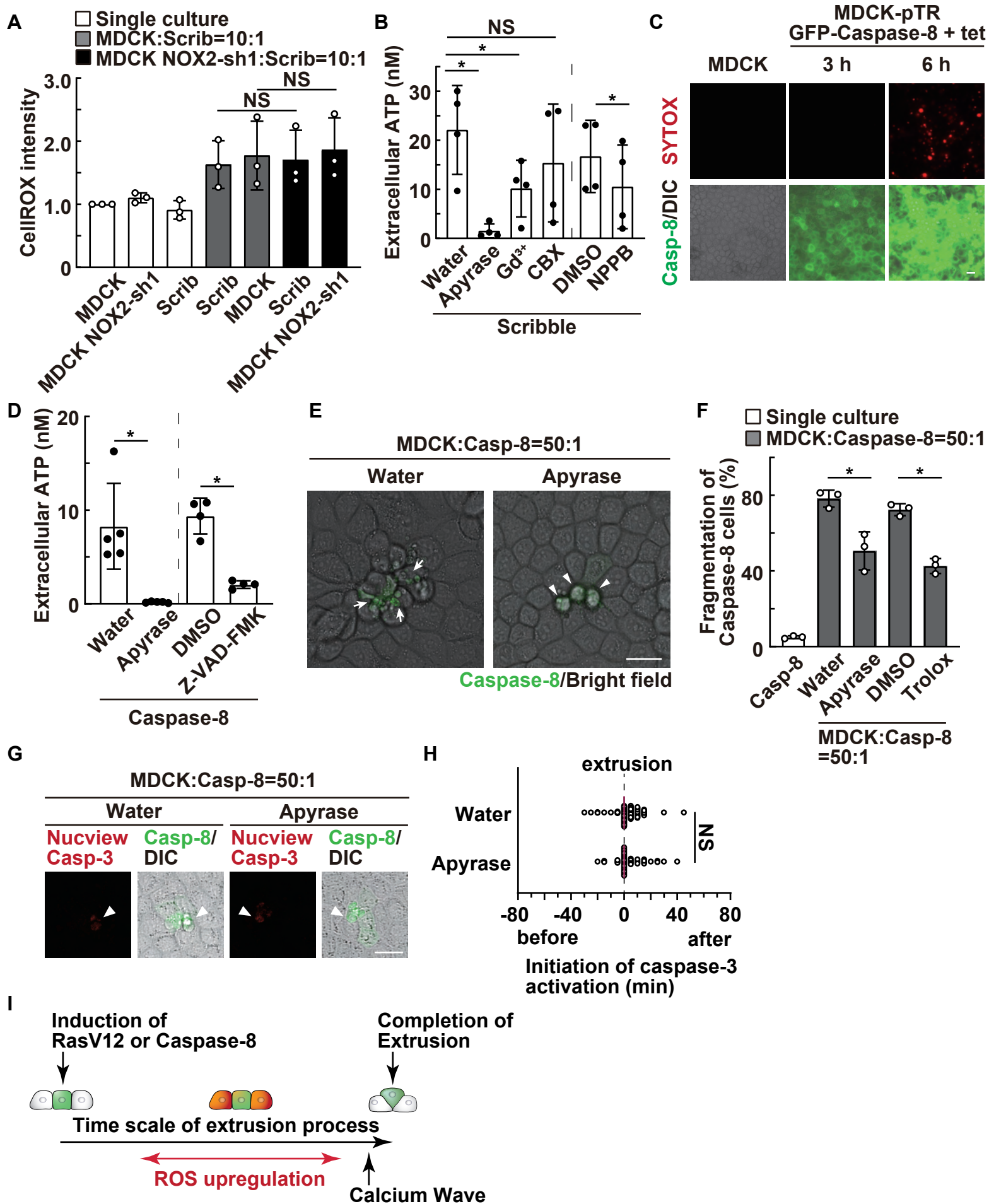Scale bars, 40 μm (A and B) or 20 μm (C).

Figure S6. Extracellular ATP and ROS pathways affect the behavior and fate of caspase-8-expressing cells surrounded by normal cells, related to Figures 5 and 6

(A) Effect of NOX2-knockdown in surrounding cells on the intracellular ROS level. MDCK-pTR Scribble-shRNA1 cells were cultured alone or co-cultured with normal MDCK or MDCK NOX2-shRNA1 cells at a ratio of 1:10, followed by CellROX analysis. Values are expressed as a ratio relative to single-cultured MDCK cells. Data are mean ± SD from three independent experiments. NS: not significant (one-way ANOVA with Dunnett's test); n = 180, 175, 180, 208, 400, 194, and 364 cells.

(B) Effect of an inhibitor for ATP release channel on the extracellular ATP level of Scribble-knockdown cells. MDCK-pTR Scribble-shRNA1 cells were treated with apyrase, Gd^{3+}, CBX, or NPPB, and the extracellular ATP level in conditioned media was measured using CellTiter-Glo 2.0 reagent. Data are mean ± SD from four independent experiments. $*p < 0.05$ and NS: not significant (one-way ANOVA with Dunnett's test (left four) or paired two-tailed Student's t-test (right two)).

(C) Effect of caspase-8 expression on the membrane integrity. Normal MDCK cells or MDCK-pTR GFP-caspase-8 cells were cultured alone, followed by the treatment with tetracycline for 3 or 6 h. Cells were then stained with SYTOX-dye to analyze the membrane integrity.

(D) Effect of apyrase or Z-VAD-FMK on the extracellular ATP level of caspase-8-expressing cells. MDCK-pTR GFP-caspase-8 cells were treated with apyrase or Z-VAD-FMK, and the extracellular ATP level in conditioned media was measured using CellTiter-Glo 2.0 reagent. Data are mean ± SD from five (Water- or apyrase-treated) or four (DMSO- or Z-VAD-FMK-treated) independent experiments. $*p < 0.05$ (paired two-tailed Student's t-test).

(E and F) Effect of apyrase or Trolox on the fragmentation of caspase-8-expressing cells within an epithelial monolayer. (E) Representative images of caspase-8-expressing cells treated with apyrase. MDCK-pTR GFP-caspase-8 cells were co-cultured with normal MDCK cells in the absence or presence of apyrase. Images were extracted from a representative time-lapse analysis (Videos S1 and S2). The arrows or arrowheads indicate fragmented or intact caspase-8-expressing cells, respectively. (F) Quantification of the fragmentation of caspase-8-expressing cells surrounded by normal cells in the absence or presence of apyrase or Trolox. Data are mean ± SD from three independent experiments. *$p < 0.05$ (paired two-tailed Student's t-test); n = 94, 177, 158, 130, and 170 cells.

(G and H) Effect of apyrase on caspase-3 activation in caspase-8-expressing cells surrounded by normal cells. (G) Representative images for the caspase-3 activity indicator Nucview. Normal MDCK and MDCK-pTR GFP-caspase-8 cells were co-cultured at a ratio of 50:1 in the absence or presence of apyrase, followed by the time-lapse observation. The activity of caspase-3 was monitored using Nucview. Arrowheads indicate caspase-8-expressing cells upon extrusion just prior to fragmentation. (H) The timing of initiation of caspase-3 activation in caspase-8-expressing cells extruded with the fragmentation phenotype in the absence or presence of apyrase. Red bars indicate median values. NS: not significant (Mann-Whitney test); n= 85 and 45 cells from three independent experiments.

(I) A schematic of the time scale of the extrusion process of RasV12-transformed or caspase-8-expressing cells from the epithelial layer.

(C, E, and G) Scale bars, 20 μm.

Inhibitors	Targets	ROS level	Apical extrusion
α-GA	gap junction	No effect	↓*
GsMTX	mechanosensitive calcium channel	No effect	↓*
Ibuprofen	cyclooxygenase	No effect	↑*
Trolox	ROS	↓*	↓*
Y27632	Rho kinase	No effect	↓*
Blebbistatin	Myosin-II	No effect	↓*
BAY117082	NF-κB	No effect	ND
VAS2870	NADPH oxidase	↓*	↓*
CCCP	mitochondrial oxidative phosphorylation	No effect	ND
Nocotazole	microtubule	No effect	↓*
CK666	Arp2/3 complex	No effect	↓*
SMIFTH2	formin	No effect	↓*
ML141	Cdc42	No effect	ND
H89	PKA	No effect	ND
U0126	MEK	No effect	↓*
LY294002	PI3K	No effect	↓*
Apyrase	extracellular ATP	↓*	↓*
Suramin	P2Y, P2X receptor	↓*	↓*
AgNO₃	Aquaporin	No effect	ND
GW4869	exosome biogenesis/ release	No effect	ND

Table S1. Effects of various inhibitors on the ROS level and apical extrusion, related to Figures 1-3

Normal MDCK cells were co-cultured with MDCK-pTR GFP-RasV12 cells at a ratio of 50:1 in the presence of the indicated inhibitor. *Statistically significant (paired two-tailed Student's t-test or one-way ANOVA with Dunnet's test); ND: not done; gray box: the indicated data are based on our published observations.